

Elsevier Editorial System(tm) for Science of
the Total Environment

Manuscript Draft

Manuscript Number: STOTEN-D-16-05999

Title: Geomorphodiversity Index: Quantifying the Diversity of Landforms
and Physical Landscape

Article Type: VSI: Mapping the Environment

Keywords: Geodiversity, Quantitative Model, Digital Elevation Model,
Central Italy.

Corresponding Author: Dr. Laura Melelli, Ph.D.

Corresponding Author's Institution: University of Perugia

First Author: Laura Melelli, Ph.D.

Order of Authors: Laura Melelli, Ph.D.; Francesca Vergari, Ph.D.; Luisa
Liucci, Ph.D.; Maurizio Del Monte, Professor

Abstract: The physical landscape is the mosaic resulting from a wide
spectrum of environmental components. The landforms define the variety,
or diversity, of the geomorphological component: the geomorphodiversity.
Landforms are usually represented in thematic maps where the scale and
the graphic solutions are widely heterogeneous. Since geomorphological
maps are not always easy to obtain and standardize, topography might be
used as a proxy to infer the morphological signature. To recognize,
evaluate, and, in some cases, promote the geomorphodiversity of an area,
a numerical assessment is preferable. A quantitative approach allows for
the comparison of different morphological environments and exploits the
topographic attributes derived from Digital Elevation Models. The aim of
this work is to define a quantitative index tested on the Umbria region
(Central Italy), a territory well known for its geoheritage.

Suggested Reviewers: Emmanuel Reynard

University of Lausanne Faculty of geosciences and environment
emmanuel.reynard@unil.ch

Prof. E. Reynard is Chair of the Working Group on "Geomorphosites" in the
International Association of Geomorphology.

Zbigniew Zwoliński

Institute of Geoecology and Geoinformation , Adam Mickiewicz University
zbzw@amu.edu.pl

Prof. Zwoliński is Chair of the Working Group on
"Landform Assessment for Geodiversity" in the International Association
of Geomorphology.

Nenad Buzjak

Faculty of Science, Department of Geography, University of Zagreb
nbuzjak@geog.pmf.hr

One of the topic research of Prof. Buzjak is the geoheritage assessment.

Marco Giardino

Earth Sciences Department, University of Torino

marco.giardino@unito.it

Prof. Marco Giardino is Chair for the Working Group "Landform Assessment for Geodiversity" of the International Association of Geomorphology (IAG)

Paola Coratza Ph.D.

University of Modena and Reggio Emilia

paola.coratza@unimore.it

Prof. P. Coratza is Chair in the "Geomorphosites" Working Group in the International Association of Geomorphology.

Opposed Reviewers:



UNIVERSITA' DEGLI STUDI DI PERUGIA
DIPARTIMENTO DI FISICA e GEOLOGIA
Piazza dell'Università – 06100 PERUGIA

Laura Meelli

Department of Physics and Geology

Via A. Pascoli, snc

Tel.: +39 075 5849579

Fax.: +39 075 5852603

e-mail: laura.meelli@unipg.it

URL: http://www.unipg.it/~lmeelli/

*Science of the Total Environment
Chief Editor*

Perugia, November 06, 2016

Subject: Submission of a research paper

With regard to the manuscript:

Geomorphodiversity Index: Quantifying the Diversity of Landforms and Physical Landscape

Laura Meelli*, Francesca Vergari, Luisa Liucci, Maurizio Del Monte

*University of Perugia - Department of Physics and Geology

Dear Editor,

as suggested by Prof. Sebastiano Trevisani, we would like to submit this research paper for the special issue “ Mapping the Environment”.

The Geodiversity and, more particularly, the Geomorphodiversity is a new and promising approach in the Earth Sciences in order to evaluate the value of the abiotic parameters in a physical landscape.

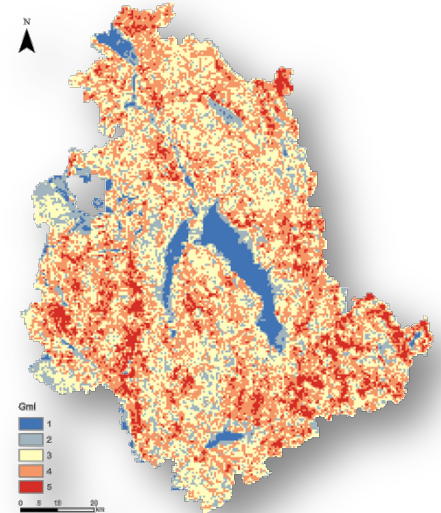
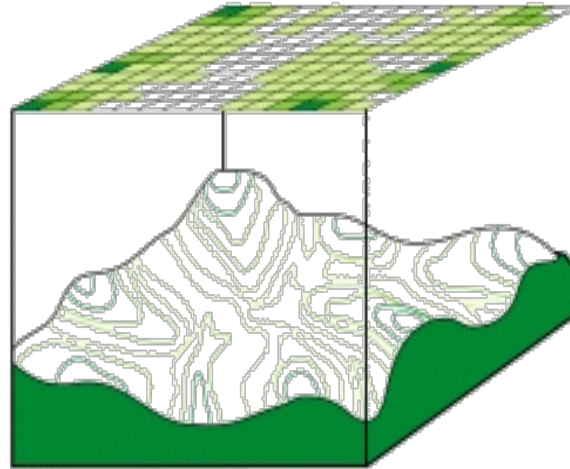
The idea of this paper is to find a digital index for evaluating the geomorphodiversity getting a numerical method in a GIS environment. The input parameters in the index evaluation are related to Lithosphere and Hydrosphere. Moreover the geomorphological features are the result of the Atmosphere and Anthroposphere too.

The Geodiversity is the necessary condition for Biodiversity and for this reason is strictly connected with the Biosphere.

One of the results of this study is a thematic map of the Geomorphodiversity Index and, more in detail, the geographical areas where the highest values of the index are present, are highlighted in density maps. So that, for being a terrain value, mapping the areal extent is the most efficient method in order to show the result of this research.

Hoping to having hit the journal's subject areas, we look forward to hear from you soon.

Best Regards,
Laura Meelli



Landscape
Landforms



GIS
analysis



Mapping
Geomorphodiversity

*Highlights (for review)

- The landscape is a mosaic resulting from a wide spectrum of environmental components.
- The geomorphodiversity includes the geological and morphological variety of the landscape.
- A numerical index (Gml) is preferable to compare different geographical areas.
- Gml is a central instrument to assess the environment in a multidisciplinary method.

1 1. Introduction

2 In the last decades many researchers have focused their attention on the definition of
3 geodiversity and its relationships with biodiversity, natural environment conservation,
4 ecosystem services, geotourism (Gray, 2004). Evaluating the diversity of an ecosystem
5 involves the necessity to define indexes able to compare different geographical and
6 morphological areas. The concept of the physiographic unit is one the main focal points
7 defining the relationships between the different variables composing the landscape (Bailey,
8 2009, Fenneman, 1916; Hooson, 1968; Miliareisis and Argialas, 1999). Fennemans' method
9 (1916), still acceptable in the scientific literature, classifies the United States in
10 physiographic provinces, and was the basis for many other studies developed for other
11 countries. Since the beginning of the 20th century the concept of physiography was enlarged,
12 including the more general idea of a geographic division of the landscape. The approach of
13 a division of the terrestrial surface in homogenous districts characterized by particular
14 processes and landforms is still a main topic for the earth scientists. To classify and divide
15 areas with similar geomorphological arrangement is the basis for a correct planning of the
16 territory for management and exploitation.

17 To this end spatial analysis and quantitative measurements of environmental variables are
18 the basis for an innovative approach to investigate the mutual relationships between the
19 different components of an ecosystem (Bétard, 2013; Hjort and Luoto, 2010; Hjort et al.,
20 2012). Abiotic and biotic components are related to each other, but methods and techniques
21 used for their assessment are not always comparable (Matthews, 2014). It is well recognized
22 that the biotic richness and the diversity of an ecosystem, or biodiversity, strictly depends on
23 the abiotic elements belonging to the same area. The geological substrate and the

24 topographic setting, together with the morphological processes and the climatic conditions,
25 create the basis for the weathering activity and the soil formation at the bottom of each biotic
26 cycle (Musila et al., 2005). Accordingly, the definition and evaluation of the abiotic
27 components is an essential step in order to compare and model the ecosystem evolution.
28 Thus, since the last decade, the scientific community has started developing a specific field
29 of research in the Earth Sciences aimed at the definition and measurement, in a quantitative
30 perspective, of the diversity of the abiotic components, or geodiversity.

31 The geodiversity of an area is defined as its “natural range (diversity) of geological (rocks,
32 minerals, fossils), geomorphological (landforms, physical processes) and soil features”
33 (Gray, 2004). The definition collects the three main abiotic components involved in
34 landscape modelling: 1) the geological parameters, 2) the geomorphological processes and
35 3) the landforms and the resulting soil types, which are the starting conditions for the biotic
36 cycles. In this qualitative characterization, no reference is given to how and how much these
37 parameters need to be taken into account when studying an ecosystem.

38 Recent works focused on a semi-quantitative approach take into account the
39 presence/absence of geosites (Reynard and Coratza, 2007) and their abundance and
40 richness as indicators of high ranks of geodiversity. Ruban (2010) suggests a further
41 clarification of the definition of geodiversity starting from the geosites, or the portions of the
42 geosphere presenting a particular importance for the comprehension of Earth history, and
43 considering their presence/absence in the study area as a measure for ranking the
44 geodiversity. A semi-quantitative definition is also proposed, where geodiversity is the sum
45 of “total quantity of geosite types occurring on a given territory” (Ruban, 2010). A complex
46 geosite, described by different components has a rank equal to the maximum value

47 observed among the counterparts' ranks. Thus, the geodiversity of an area is the sum of
48 maximum rank scores of each type of geosites within a given territory.

49 In this work the geodiversity is not evaluated based on the presence of geosites. This choice
50 is motivated by the fact that a landscape can be regarded as having a high value of
51 geodiversity without hosting any geosite. Moreover, the identification of a geosite requires a
52 specific research, also involving an in-depth knowledge about visibility, management and
53 other aspects, like cultural and aesthetic values, which are not necessary in the geodiversity
54 assessment.

55 Following the decoupling of geodiversity from geosites, the second point is how the
56 assessment of the abiotic components can be improved, moving towards a quantitative
57 evaluation. This last approach has several advantages. First of all, a quantitative approach is
58 an objective and repeatable procedure, thus allowing for the comparison of areas in different
59 geographical contexts. Second, a Geodiversity Index (GI) value can be joined to a
60 planimetric area, usually corresponding to a squared cell in a raster layer, so that large
61 areas may be tiled in zones with similar GI values. Moreover, this approach would allow
62 overlaying the GI to other spatial terrain information for different purposes. Geographical
63 Information Systems (GIS) and remote sensing data are the best tools for a quantitative
64 definition by exploiting digital terrain data (Yongxin, 2007). Geodiversity indexes have been
65 mostly implemented for regional scale studies, improving the number and quality of historical
66 cases in the recent years (Benito-Calvo et al., 2009; Hjort and Luoto, 2010; Melelli, 2014;
67 Pereira et al., 2013; Serrano and Ruiz-Flaño, 2007; Silva et al., 2015; Vergari, 2009;
68 Zwoliński, 2010). In this context, the GI has been recently correlated with a new
69 geovisualization technique in order to improve the digital cartography and the 3D virtual

70 displaying (Martinez-Graña et al., 2014; Melelli et al., 2012). Useful implementations are also
71 suggested for a wide range of purposes, such as geoparks and geoheritage characterization
72 (Erikstad, 2013; Ferrero et al., 2012; Panizza and Piacente 2009) or for hazard evaluation
73 and prevention (Gordon et al., 2012).

74 The quantitative procedure for the GI assessment generally takes into account several
75 terrain parameters, such as the geological, geomorphological, hydrographical and
76 topographic datasets. Among these, the geomorphological data are the most difficult to
77 include in an automatic procedure. Although geomorphological mapping production is
78 aligned with new digital techniques (Gustavsson et al., 2006), currently the
79 geomorphological characteristics are still the most difficult to obtain, in particular due to the
80 lack of geomorphological maps for large areas. Moreover, the geomorphological information
81 is extremely complex to be represented due to the huge amount of associated data, thus
82 resulting in a map that is not easily converted to a digital format (Carton et al., 2005; Melelli
83 et al., 2012). The large heterogeneity of symbols and legends used to represent landforms
84 and their close dependence on the scale is one of the strongest barriers preventing the use
85 of geomorphological datasets. Further, geomorphological mapping has a no continuous
86 drawing. Symbols representing landforms are interposed with blank – empty space and in
87 some cases the same area includes more than one landform.

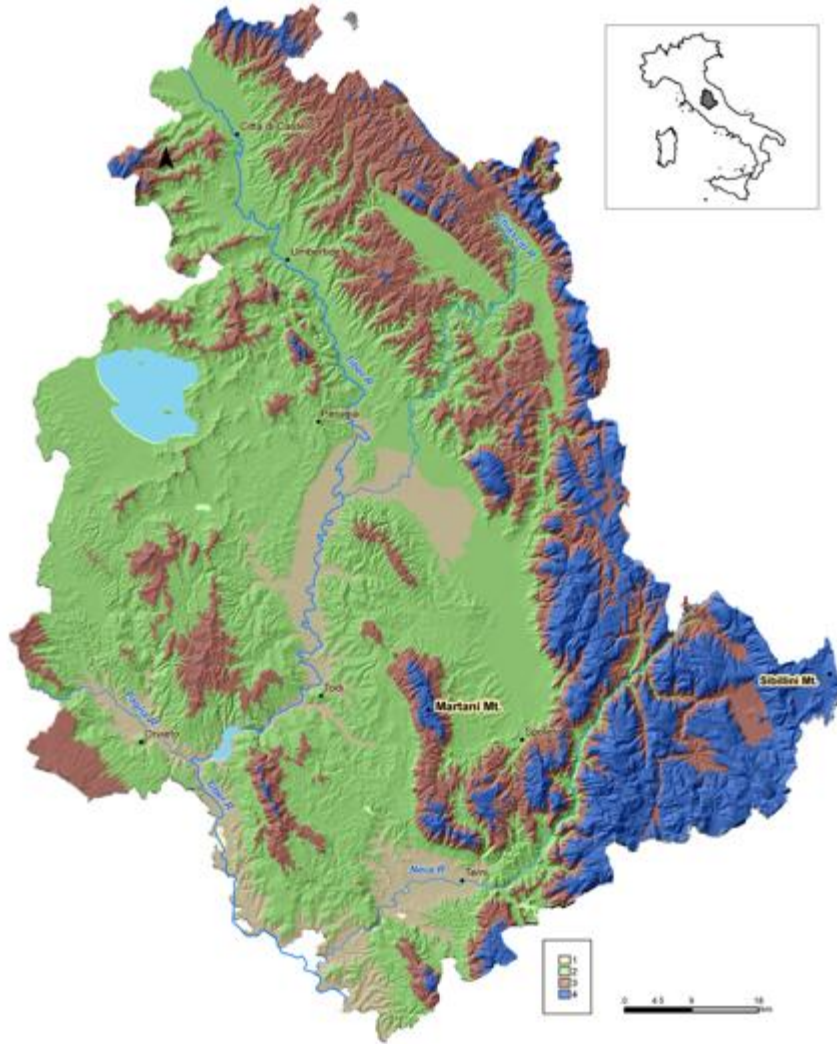
88 Some geodiversity models already applied to Italian regional territories (e.g. Vergari, 2009)
89 present some limits essentially due to i) the low number of components considered to
90 assess geodiversity (i.e. those models in which the analysis is only limited to the lithology
91 diversity) and ii) the a priori assignment of weights to the different geodiversity components.

92 The first purpose of this work is to elaborate a procedure that uses GIS and Digital Elevation
93 Models (DEMs) to obtain an automatic and unbiased mathematical expression for the
94 morphological component of GI, the geomorphodiversity index (Gml). The second
95 fundamental aim is to propose a digital Gml, attempting to replace the geomorphological
96 maps by the morphometric parameters derived from the elaborations of DEMs. This
97 represents the main difference between the numerical model proposed in this work and the
98 formulas already existing in the scientific literature. In this way, the proposed method uses
99 the geomorphological data only to validate the result and not as input parameters, in order to
100 avoid the above-mentioned limits of the geomorphological thematic mapping.
101 We apply our approach to the Umbria Region (Central Italy) and the results are validated
102 comparing the resulting Gml map with the available geomorphological maps of a selected
103 part of the study area, considering the geomorphology of a territory as the result of the
104 interactions among all the components contributing to define its geodiversity.

105

106 2. The study area

107 Umbria (Central Italy) is the only peninsular Italian region without access to the sea,
108 covering an area of 8,456 km² (Fig. 1). Bounded by gentle hills to the west and mountains to
109 the east, the Umbrian territory, despite its limited extent, is characterized by an outstanding
110 diversity of geomorphological and geological contexts.



111

112 Figure 1. Umbria region: location map and elevation ranges a.s.l. 1) <200m, 2) 200-
 113 500m a.s.l., 3) 500-800m, 4) >800m.

114

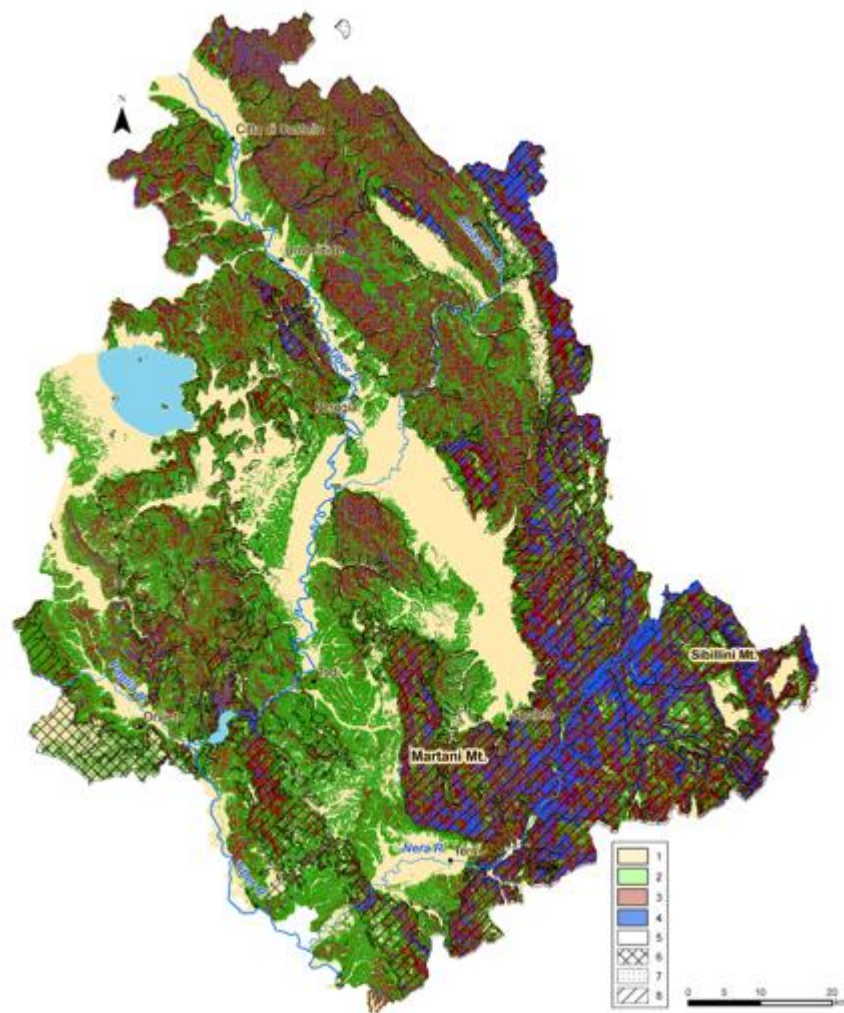
115 Climate in Umbria is Mediterranean with the exception of the innermost areas where sub-
 116 continental conditions prevail, with wet winters and dry summers. Average annual rainfall
 117 ranges from 1,000 to 1,200 mm/year. The maximum rainfall values occur in November; the
 118 minimum in July and March.

119 The hilly setting is predominant (Fig. 1), and is characterized by both low (200–500m a.s.l.

120 52% of the regional area) and high (500–800m, 24% of the total) landscapes. The first is

121 present in the entire regional area, with the exception of the north eastern sector, where the
122 high hills are prevalent, and of the southeastern portion, occupied by mountains (14% of the
123 total area, with an average altitude value higher than 800m, and the highest peak being
124 Cima del Redentore at 2448 m, in the Sibillini Mountains). The remaining 10% is below
125 200m, confined to the Terni basin and the middle and lower Tiber valley. The region is
126 longitudinally crossed by the Tiber River, starting from the northern boundary along the
127 Upper Tiber Valley with an altitude of 320m and flowing along 50 kilometres of the regional
128 territory. After a segment with a N-S direction, the Tiber River passes close to the town of
129 Perugia, where it receives one of its major left tributaries, the Chiascio River. Then, moving
130 southward, near the village of Todi, it abruptly changes its direction (NE-SW), passing along
131 the Forello Gorge (17 km long with 37 m of difference in height), where it creates the artificial
132 Corbara Lake. Further, not far from the town of Orvieto, the Tiber River receives the right
133 tributary Paglia. Then, tracing the Umbrian border for a long stretch finally enters the Lazio
134 region. Here, near the town of Orte, it receives the Nera River. The Tiber River draws
135 partially the Tiber Basin, the largest of the intermountain basins in the Umbria region (with
136 an area of about 1800 km²) with an overturned Y shape splitting near Perugia (Basilici, 1997
137 and references within). The three branches are narrow and elongated in the NS direction.
138 The northern segment is the Upper Tiber Valley (Melelli, 2014); the western one continues
139 southward to Terni, where it widens into a depression (The Terni basin). The last and
140 easternmost segment of the Tiber basin corresponds to the Umbrian Valley, running from
141 Perugia to Spoleto. Between the western and eastern segments, the ridge of the Martani
142 Mountains develops. The morphological setting agrees with the topographic setting and,
143 most of all, with the geological substrate. In Figure 2 slope values are grouped into four

144 classes highlighting a spatial distribution very similar to the altitude values mapped in Figure
145 1.



146

147 Figure 2. Correspondence between slope angle values and lithological complexes.

148 Slope angle classes: 1) 0°-5°, 2) 5°-16°, 3) 16°-30°, 4) >30°. Lithological complexes:

149 5) Fluvial lacustrine deposits, 6) Volcanic complex, 7) Terrigenous complex, 8)

150 Carbonate complex.

151

152 The lowest range (class 1, slope values between 0° and 5°, 25% of the total area) is present

153 in the main intermountain basins, along the alluvial plain and around Trasimeno Lake. A

154 second slope class (5°-16°, 41% of total area) is widespread in the whole area, mostly in the
155 western part. These topographic values correspond to the youngest sediments of the region:
156 the post-orogenic Plio-Pleistocene deposits. Marine and continental sediments with a great
157 compositional heterogeneity constitute the post-orogenic complex (Pliocene – Holocene).
158 The most represented environment is the fluvial-lacustrine, which is characterized by
159 sedimentary sequences of variable thickness, with alternating conglomerates, sands and
160 clays. The coarser fraction mainly crops out at the top of the hills; sands prevail on the side-
161 slope. The foot-slope is mainly constituted by fine sand and clay. Fluvial-lacustrine deposits
162 mainly fill the intermountain basins and the valleys of the region. Shallow and recent
163 sediments (Holocene) of alluvial origin crop out on the flat areas of the region. Eluvial,
164 colluvial and debris deposits are widely present in those zones occurring at the transition
165 between the mountainous areas and the adjacent plains.

166 The Terrigenous synorogenic complex is present where the slope values are higher, such as
167 in the third class of the slope gradient (16°-30°, 28% of total area). The highest slope values
168 (30-76°) only cover about 6% of the region and show a good correspondence with the oldest
169 Carbonate lithological complex. The Terrigenous complex (Oligocene – Medium Miocene) is
170 present in the northern and central part of the study area; it consists in a synorogenic
171 turbidite sequence of limestone and arenaceous layers interbedded with marls and clays.

172 The paleoenvironment is that typical of turbidities, thus varying from pelagic basin, to
173 continental slope, to foredeep basin. A compressive tectonic phase (Upper Miocene– Lower
174 Pliocene) affected the entire turbidite sequence, thus generating folds and thrusts dipping
175 eastward. The sequence was then involved in an extensional phase, which created sets of
176 normal faults resulting in valleys and intermountain basins. As a result of the lithological

177 diversity of this complex, the bedrock is characterized by a heterogeneous mechanical
178 behaviour, which depends on the rock permeability and on its specific response to
179 weathering and erosion. Consequently, the geomorphological evolution of the landscape is
180 highly different in the different portions of this geological complex, thus generating non-
181 homogeneous slope geometry. The relief is characterized by high amplitude values where
182 sandstone and limestone prevail; gentle slopes characterize the marl bedrock. Fluvial and
183 gravitational processes mainly consisting of slides and flows are the predominant processes
184 shaping the surface. Dendritic drainage patterns are characteristic of this complex; the
185 drainage density increases with the percentage of clay.

186 The Carbonate complex (Upper Trias – Lower Miocene) crops out continuously in the
187 southeastern portion of the region, and, with a lesser extent, in correspondence with the
188 reliefs in the central sector. Moving from the bottom to the top of the sedimentary multilayer,
189 the lithological composition changes from limestone to marl limestone. As a consequence of
190 the tectonic fragmentation that generated high and low structural domains, different
191 depositional environments characterize this complex. In particular, the paleoenvironments
192 evolved from evaporitic basin of shallow water to carbonate platform to pelagic basin. Wide
193 anticlines alternating with narrow synclines (with NW–SE or N–S direction) are the prevalent
194 tectonic style. Fault systems with two main directions, according to the Apennine and anti-
195 Apennine trends, cut the folds. Mountain chains have wide and flat tops due to both the
196 geological structures where the layers show flat attitude, and the presence of paleosurfaces
197 generated by erosional processes started during Lower Miocene – Upper Pliocene. Karst
198 landforms consisting of dolines, and eluvial deposits are also frequent in this complex. A
199 convex-creep zone followed by a convex-straight profile characterizes the upper part of the

200 slopes; gentle slopes and thick colluvial deposits are present in bedrock, where the marl
201 fraction is high. Overall, this geological complex exhibits low values of drainage density.
202 Fluvial erosion is more effective where the regional fault system and the lithological
203 discontinuities control the evolution of the river network, and it results in deep river valleys
204 and rectangular drainage patterns. Alluvial deposits are present in the riverbed of streams,
205 which flows along the syncline axes.

206 In order to complete the geological description of the region, the Volcanic complex (age of
207 600–130 ky) must be mentioned, although it only covers a limited portion in the
208 southwestern part of the area. This complex represents the north eastern edge of the Alfinia
209 plateau belonging to the Vulsini District (Margottini et al., in press) and is mainly
210 characterized by ignimbrite deposits and stratified tuffs (Peccerillo, 2005). The area consists
211 of low reliefs and gently dipping summit surfaces. The main evidence of the past volcanic
212 activity is Bolsena Lake, which occupies an ancient caldera, while a post-Miocene
213 extensional tectonic phase generated N–S and NW–SE fault systems. These resulted in
214 numerous scarps following the direction of the fault systems. The tectonic activity also
215 affected the spatial organization of the drainage network, which exhibits rectangular patterns
216 controlled by the tectonic lineaments (Ciotoli et al., 2003).

217 From the above description it is clear that the Umbria region shows a wide range of
218 topographic and morphological characteristics, related to the geological setting and to the
219 complex tectonic evolution.

220 The natural heritage is relevant, with thirty-three geosites, seven regional protected areas
221 and one national park. Due to the low population density, the physical landscape is a
222 relevant feature of the region. The natural diversity, with the contribution of the geological

223 one is the main cause for this richness.

224

225 3. Methods

226 The quantitative index, which we propose, is based on the concept of geomorphological
227 diversity or geomorphodiversity (Thomas, 2012), thus restricting the input data only to those
228 variables associated with the evolution of the physical landscape.

229 In order to parameterize the processes shaping the Earth surface, topographic attributes
230 must be necessarily considered. It is natural, therefore, to rely upon methods and data that
231 can be directly derived from the geomorphometric analysis of Digital Elevation Models
232 (Evans, 2013; Pike, 2000). The primary and secondary attributes useful for landform
233 representation such as slope, aspect, curvature and roughness are extensively described in
234 the scientific literature (e.g. Bétard, 2013; Melelli and Taramelli, 2010; Taramelli and Melelli
235 2009a, 2009b; Wu et al., 2008). However, the information associated with these attributes in
236 some cases is rather similar. As a result not all these attributes are included in the analysis
237 not to overload the procedure with redundant data. Because of this, a pre-analysis was done
238 crossing-comparing the most used topographic attributes for the study area and analysing
239 their correlation. In particular, the curvatures (both the planar and the radial) are discarded
240 from the input data because, as discussed in Section 4.3, they show behaviour similar to
241 roughness. The remaining factors, selected in the pre-analysis, are all included in the
242 formula for the index characterization.

243 All these variables are analysed and managed in the GIS environment, using the spatial
244 investigation in map algebra with tools and functions useful for geographical analysis.

245 The applied mathematical expression (1) is the sum of five factors; all of them are grids of
 246 different terrain parameters. A grid is a spatial geographic data format, i.e. a raster image
 247 where each pixel is equivalent to a “cell” with a physical parameter associated to it (Fig. 3).

248

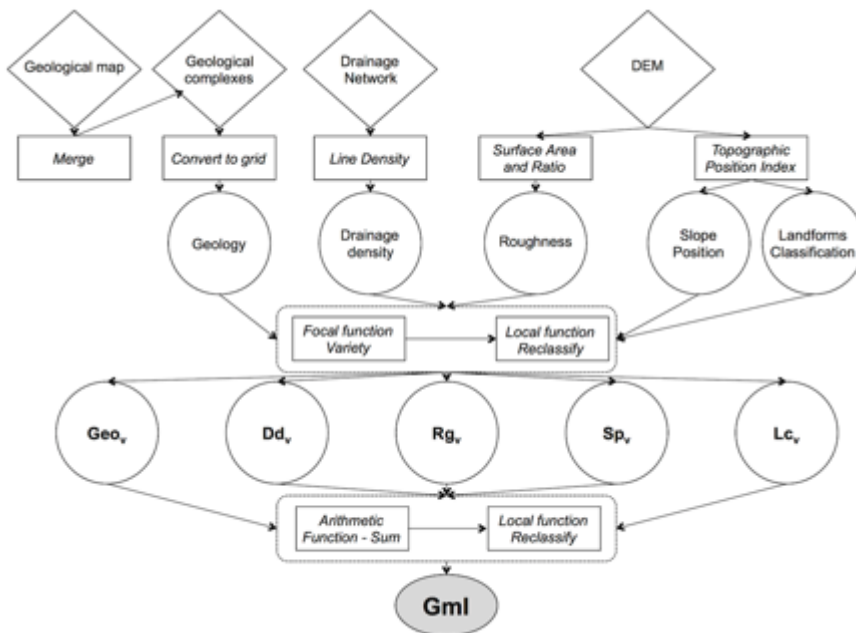
$$249 \quad GmI = Geo_v + Dd_v + Rg_v + Sp_v + Lc_v$$

250 (1)

251

252 Where

- 253 • GmI is the Geomorphodiversity Index,
- 254 • Geo_v is the classified raster map of geological diversity factor,
- 255 • Dd_v is the classified raster map of the drainage density diversity factor,
- 256 • Rg_v is the classified raster map of the roughness diversity factor,
- 257 • Sp_v is the classified raster map of the slope position index diversity factor,
- 258 • Lc_v is the classified raster map of the landform category diversity factor.



259

260 Figure 3. Flow chart showing the steps of the analysis.

261 Terrain data are derived from the DEM as a floating raster (Rg_v , Sp_v Lc_v) or converted into a

262 grid raster from a starting vector layer (Geo_v , Dd_v). Two functions are used: the focal

263 function, and the local one (ArcGIS 10.x © ESRI).

264 In order to evaluate the diversity of each parameter, a neighbourhood statistic function is

265 applied. The focal function computes an output raster where the value at each location

266 depends on the values of the input cells in a specified neighbourhood of that location. A

267 moving window, where the statistical value is computed, defines the neighbourhood.

268 Different statistic parameters can be used to obtain the output values, such as the

269 maximum, mean, range or Standard Deviation (STD) of all the values present in a given

270 mask. In Eq. 1 the statistical value used is the variety. This parameter defines the diversity of

271 the values (the number of unique values) on a cell-by-cell basis within the analysis mask.

272 The output is always an integer grid. The analysis mask can be defined as a rectangle of

273 any dimension, a circle or annulus of any radius or an oriented wedge in any direction. The

274 dimensions of each geometric figure are in cells or map units. The selected mask is a circle.

275 The radius value is identified in map units in order to obtain a circle area equivalent to 1

276 square kilometre. The radius is selected considering a meaningful area comparable to the

277 DEM resolution and suitable for the aim of the analysis. Even if a rectangle mask produces

278 the best resolution enhancement, this shape also creates a blocky-looking output that results

279 from the fact that peaks or sinks are included (Guzzetti and Reichenbach, 1994). In order to

280 avoid this disadvantage, the circle optimizes an omnidirectional resolution.

281 Therefore, for each terrain parameter the grid of variety is computed and, in order to assign

282 the same weight to each parameter, a reclassification in five classes is done. The choice to

283 use five classes is the final result of several attempts where the qualitative geomorphological
284 information is compared with the resulting areas of the reclassification. With five classes the
285 cells are properly grouped, representing homogenous areas with the same characteristics in
286 terms of geomorphodiversity. A lower number of classes limits the diversity inside some
287 areas where, on the contrary, a large variety is well known. A higher number of classes
288 changes the aim of the procedure, which is to group the cells to highlight areas with
289 homogeneous characteristics in terms of geomorphodiversity.

290 This procedure ensures that the range of classes is equal for all the parameters. The
291 statistical method used to classify each dataset is the Jenk's natural breaks algorithm, which
292 clusters the data values based on their distribution (Jenks, 1967). The algorithm reduces the
293 variance within groups and maximizes the variance between them.

294 The final sum of the input raster data is then performed. The sum provides the GI value of
295 an area. To obtain this value it is not necessary to use a weighted overlay, since the
296 reclassification, according to Jenks algorithm, has already assigned the proper rank to each
297 class of each input parameter.

298 The sum assigned the same rank to each input parameter according to Jenks algorithm. In
299 the final sum, the cell size is lowered to the minimum value of all the terrain parameters, i.e.
300 500m. The choice of lowering the cell size is made by taking into account the resolution of
301 the data entries, in order to increase the reliability of the output data. With this approach in
302 mind, it is preferable to reduce the initial data with high spatial resolution rather than
303 increasing the lowest ones.

304

305 4. Input data

306 4.1 Geological vector (Geo_v)

307 In order to obtain a geomorphodiversity index, which is capable to express the effects of
308 modelling processes on the relief, it is necessary to consider a factor expressing the spatial
309 variation of the main bedrock characteristics. For this reason a geological factor has been
310 added to the input data.

311 The geological layer has been extracted from the official vector geological map of the
312 Umbria Region ([http://www.regione.umbria.it/paesaggio-urbanistica/cartografia-geologica-](http://www.regione.umbria.it/paesaggio-urbanistica/cartografia-geologica-informatizzata-vettoriale)
313 [informatizzata-vettoriale](http://www.regione.umbria.it/paesaggio-urbanistica/cartografia-geologica-informatizzata-vettoriale)) stored in a GeoDataBase (ESRI © model). The shapefile,
314 completed in 2012, derives from field surveys at scale 1:10.000. The original vector data has
315 a total of 46982 features, being the subdivision of the outcropping lithotypes and sediments
316 hierarchically organized.

317 The litostratigraphic units are split in formations and members. The sediments are grouped
318 into chronostratigraphic units defined by unconformity-bounded regional bodies:
319 supersynthems, synthems and subsynthems. The characteristics related to the response in
320 terms of geomorphodiversity assessment are the geological properties that are relevant to

321 morphogenetic processes. Consequently, the outcrops have been grouped according to the
322 type of rock or sediments and properties in term of topographic response (cohesion,
323 permeability, tectonic style) to erosion processes. This grouping does not take into account
324 the chronostratigraphic data and merge the levels considering only the properties relevant
325 for the index assessment.

326 In this way seven classes have been obtained:

- 327 • Alluvial deposits constrained to river tracks on flat areas,
- 328 • Debris and Fluvial deposits (mainly gravels),
- 329 • Fluvial and lacustrine deposits (mainly sands),
- 330 • Fluvial and lacustrine deposits (mainly clays),
- 331 • Terrigenous Complex,
- 332 • Carbonate Complex,
- 333 • Volcanic Complex.

334 The final shape file is converted to a grid with a cell size of 25m. Then, the diversity of the
335 values is computed, obtaining an integer grid that is a raster format where a terrain value is
336 assigned to each pixel, or cell. It was then reclassified in five classes and the break values
337 were identified according to the Jenks algorithm.

338

339 4.2 Drainage Density (Ddv)

340 While topographic attributes and the derived indexes are adequate to highlight the
341 geomorphological diversity in mountains and hilly areas, they fail in the flat ones. On plain
342 territories, the low or null difference in altitude decreases the efficiency of topographic
343 attributes to describe morphometric characteristics.

344 The flat regions of the study area correspond to alluvial plain crossed by several rivers and
345 streams. In active alluvial plains the morphogenetic processes can be fast, especially near
346 the stream channels, developing a large number of erosional and depositional landforms.
347 Hence, the drainage network may be a valid input parameter, useful for geomorphodiversity
348 assessment.

349 In order to find an efficient numerical attribute to link the presence/absence of the river
350 network to the geomorphology, the Drainage density (Dd) is considered (Tucker et al.,
351 2001). The Drainage density parameter (Horton, 1945) is a function of erodibility and
352 permeability and, therefore, it can be also connected to the degree of fracturing. Many
353 studies on the spatial variation of the Dd values highlighted their usefulness in identifying
354 zones with different geological and geomorphological characteristics (Del Monte 1996; Lupia
355 Palmieri et al., 2001; Strahler 1958). The Dd, defined as the total length of the entire river
356 network in a drainage catchment divided by the area of the basin, also depends on climatic
357 conditions, slope angle, land use and landcover. Thus, it is an excellent parameter to identify
358 and highlight the relationships between the hydrographical component and the
359 geomorphological characteristics of an area.

360 Rather than to extract the rivers from the DEM with an automatic procedure (Hydrological
361 analysis tools © ESRI), we preferred to digitize the drainage network from the topographic
362 maps with an equivalent scale (1:25.000). Even if the digitalization is strictly dependent on
363 the spatial scale, it produces more reliable results on flat areas. The automatic procedures,
364 instead, typically fail where the flow direction and accumulation are not well emphasized by
365 clear differences in altitude, such as on flat areas. Furthermore, the algorithm may not
366 consider neither the artificial channels, which sometimes do not follow the maximum slope

367 direction, nor the meandering rivers with a radius of curvature lower than the cell size of the
368 DEM. These approximations result in an underestimation of the total length of the drainage
369 network. Considering that the alluvial plains are just the portions of the study area where Dd
370 should improve the GI index, we preferred to rely upon input data with a higher level of
371 accuracy.

372 In this way, a polyline vector layer was obtained. The topological relationships between the
373 segments of the networks are added by converting the shape into a 3D vector layer. To
374 compute the Dd value, the Line density Tool in ArcGIS was used. The magnitude per area
375 unit is derived from the polyline features (rivers) falling within a given radius around each
376 output raster cell, thus obtaining, as output, a grid data. Density is calculated in units of
377 length per unit area, similar to the Dd parameter. Several values were tested for the radius in
378 order to find the optimal resolution in an output grid with a cell size of 500m. This spatial
379 resolution has been chosen since it is the lowest one among those of the data entries. Once
380 again it is important to highlight that Drainage Density is added in the Gml evaluation mostly
381 to better define the diversity of the geomorphological aspect on flat areas. Where the
382 topographic model is quite monotonous and the climatic conditions allow it, the fluvial
383 process is the most important factor favouring and increasing geodiversity.

384 4.3 Roughness (Rgv)

385 The topographic attributes derive from a DEM with a cell size of 25x25m. The terrain model
386 is obtained from the digitalization and interpolation of contour lines and spots heights drawn
387 on topographic maps with similar resolution. The altitude values are interpolated in order to
388 obtain a grid DEM (more details about the procedure may be found in Taramelli et al., 2008).

389 The landscape roughness is the measure of how a topographic surface is irregular (Hani et
390 al., 2011). In a geomorphometric approach, roughness can be based on different
391 topographic attributes, such as the standard deviation of slope or elevation. In this context,
392 and with the purpose of avoiding redundant data in the calculation of the Gml index, the
393 roughness was compared with other topographic attributes in a pre-analysis phase, through
394 the use of a multivariate analysis. The topographic attributes taken into account were the
395 slope angle, the planar and the radial curvature. This analysis was performed using the
396 Collection Statistics tool, which provides statistics for the multivariate analysis of a set of
397 raster. Together with the basic statistical parameters, the use of the “Compute covariance
398 and correlation matrices” option also returns, as outputs, the covariance and correlation
399 matrices. Results obtained from this procedure highlighted a good correlation between the
400 roughness and the slope, the planar and radial curvatures, thus indicating that the
401 roughness is capable of describing the spatial range of all these parameters. Based on
402 these results, both the slope and the curvature were discarded for the computation of the
403 Gml. Roughness is strongly affected by the scale, since the concept of roughness may be
404 applied on a multi-scale level (Hollaus et al., 2011). In this study roughness was computed in
405 a grid format as the ratio between the real surface area and the planimetric one of the same
406 square cell (Jenness, 2004). High values of roughness identify zones where valleys and
407 ridges are frequently alternated and are associated with heterogeneous geological substrate
408 or with an intense geomorphological activity (Melelli, 2014). Therefore, the higher the value
409 of roughness, the higher the probability to detect landforms. The surface area for a cell is
410 calculated considering the elevation of that cell plus the elevations of the 8 adjacent cells
411 (Jenness, 2004). A 3-dimensional space is built starting from the centerpoints of each cell,

412 achieving nine columns with height proportional to the elevation value of each cell. Then the
413 Euclidian distance between the focal cell's centerpoints and the centerpoints of each of the
414 eight surrounding cells is calculated. It is important to highlight that this distance is not the
415 planimetric one, being in a 3D space. A triangulation is performed using the centerpoints as
416 vertices and the distances as sides. By limiting the area values only to the portion of the
417 triangles lying within the cell boundaries, the surface area for that cell is estimated (Jenness,
418 2004).

419 4.4 Slope position index (Sp_v) and Landform category (Lc_v)

420 The last two addends in the Gml formulation derive from a common morphometric value
421 defined as a Topographic Position Index (TPI; De Reu et al., 2013; Weiss, 2001). The TPI is
422 defined as the difference between a cell elevation value and the average elevation on a
423 neighbouring area around the cell. Positive TPI values are associated with cell elevations
424 higher than the surrounding, inside the mask analysis; negative TPI are associated with the
425 lowest and near zero elevations in flat areas. TPI is scale-dependent; thus, attempts must be
426 made to find the best resolution for the analysis. The final classification, based on Sp and
427 Lc , depends on the scale used to analyse the landscape.

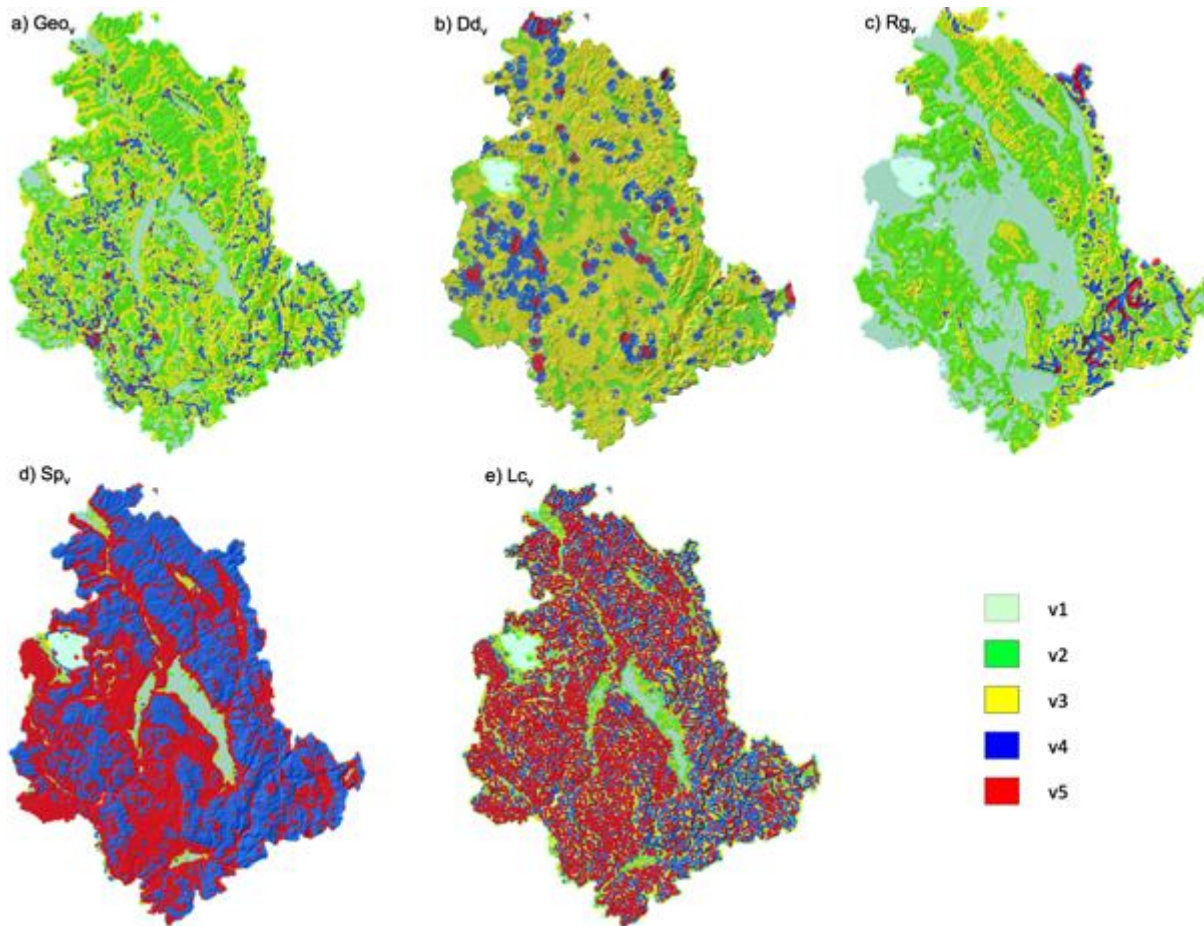
428 The TPI is computed considering a 100 m radius circle neighbourhood. Thresholding the TPI
429 values at a given scale and pointing out the slope values near zero, slope position classes
430 (Sp_v) can be extracted. In our analysis the threshold of 100m is the same of the TPI grid and
431 the slope position classes are six, distinguished in: valley, lower slope, flat slope, middle
432 slop, upper slope and ridge. The TPI values below the threshold are classified as valley or
433 lower slope, while those above the threshold are classified as upper slope and ridge. Flat
434 slope and middle slope are the classes for TPI values near zero. Comparing the TPIs

435 obtained at two different scales derives a further index. A set of rules is used for determining
436 how landform values may be classified. The resulting grid is a Landform category (Lc_v). In
437 our analysis the scale range is between 500m and 1,000m cell size maps. The detected
438 landforms are grouped into ten classes. In the first class canyons and deeply incised
439 streams are present; in the second one, midslope drainages and shallow valleys are
440 considered. Upland drainage and headwaters, U-shaped valleys, plains, open slope, upper
441 slopes and mesas, local ridges and hills in valleys, midslope ridges and small hills in plains,
442 mountain top and high ridges are the other eight classes. For both Sp and Lc the focal
443 function of variety is applied and the resulting grids are classified into 5 classes.

444

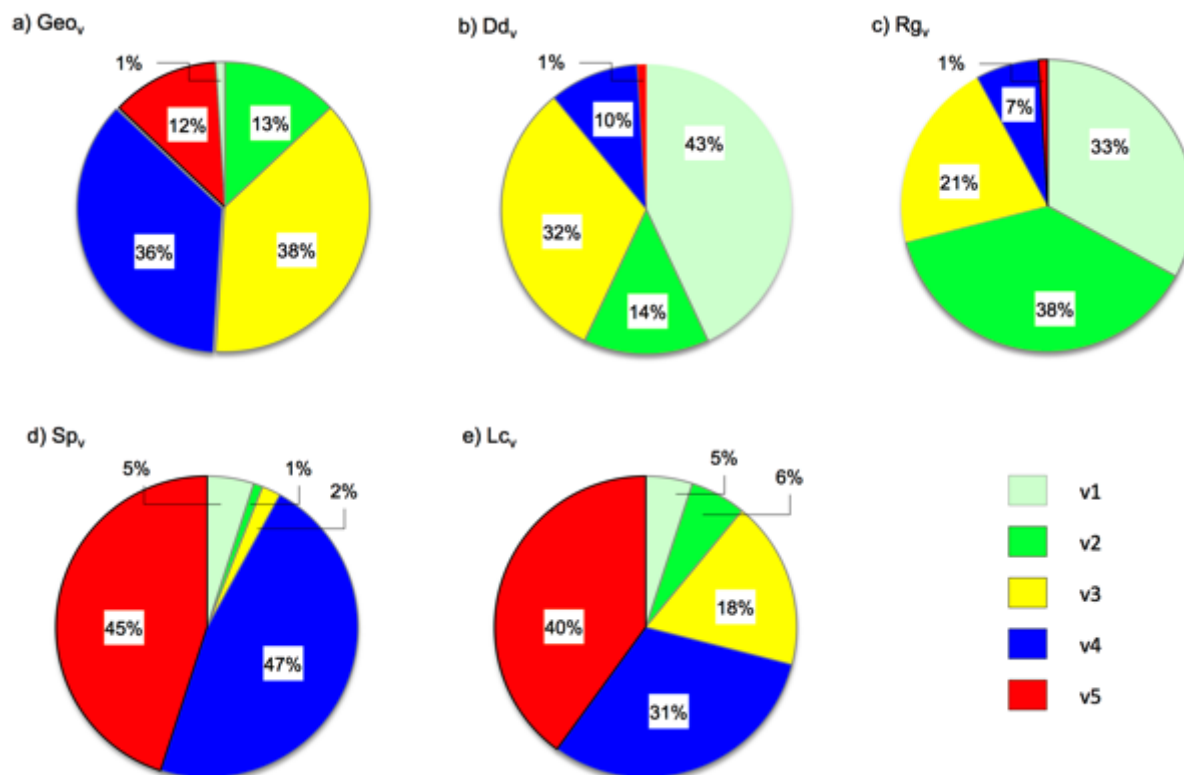
445 5. Results: the Gml map

446 The Gml is the sum of the variety of each terrain parameter taken into account. Each variety
447 grid is classified into five classes in order to attribute the same weight to each parameter in
448 the final sum (Figs. 4 and 5).



449

450 Figure 4. Variety maps in grid format. a) Geological factor, b) Drainage density, c)
 451 Roughness, 5) Slope position, 6) Landform category. Colours indicate the variety,
 452 which increases from class v1 (lowest) to class v5 (highest).



454

455 Figure 5. Pie charts showing the percentages of each variety class for the maps
 456 shown in figure 4. a) Geological factor, b) Drainage density, c) Roughness, 5) Slope
 457 position, 6) Landform category. The colours indicate the variety which increases from
 458 class v1 (lowest) to class v5 (highest).

459

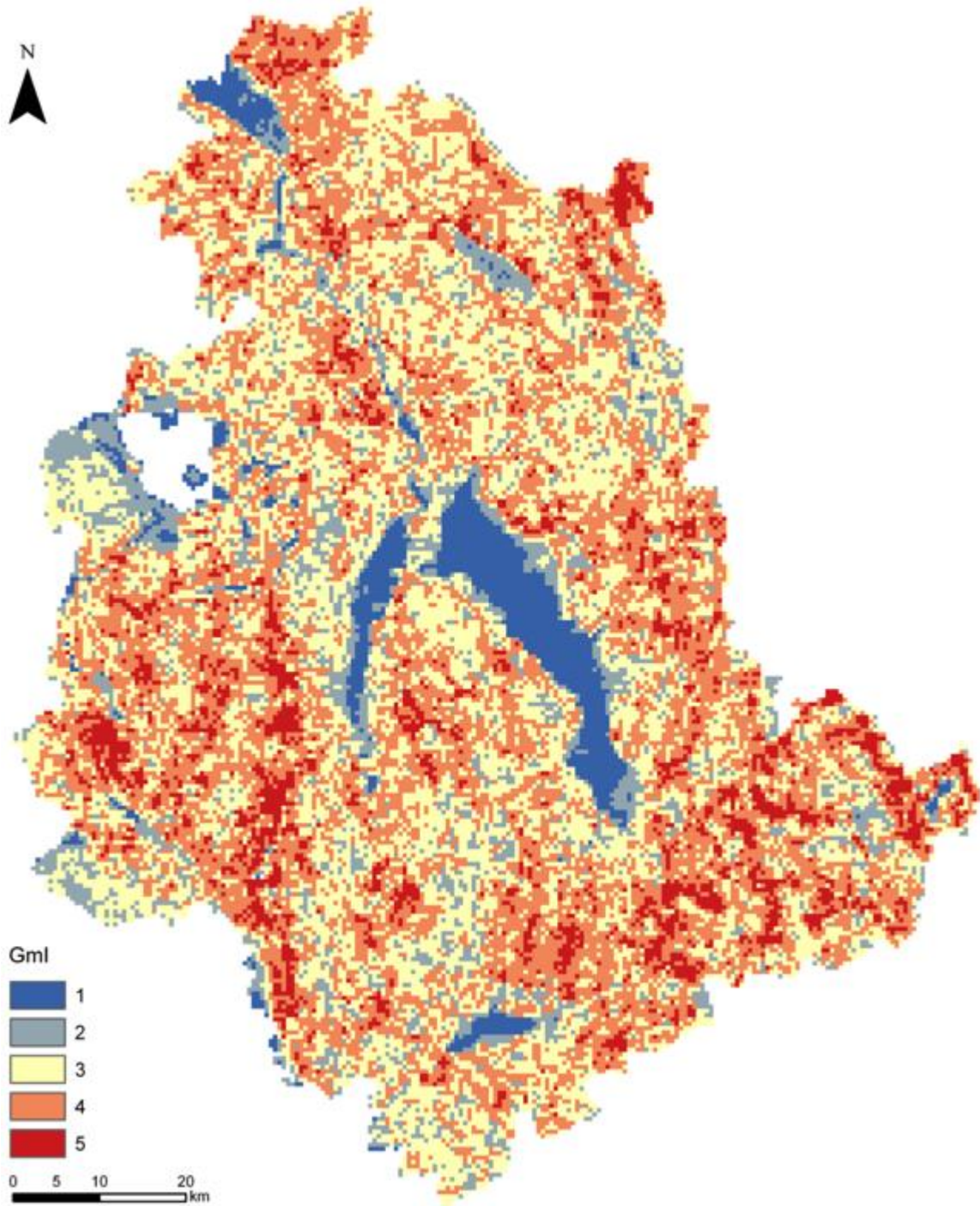
460 The percentage of the variety classes is: variety (v) v_1 (lowest), 12% of the total area; v_2 ,
461 38%; v_3 , 36%; v_4 , 12%; v_5 (highest), 2%. The lowest values (v_1 and v_2) are distributed along
462 the larger valleys and where the Terrigenous complex is more extended (northern part of
463 Umbria), the highest values (v_3 and v_4) are uniformly distributed in the rest of the study area
464 with some spots of v_5 along isolated zones on the southwestern portion of the Umbria
465 region.

466 The Drainage density variety (Dd_v) classifies the original data into five classes, where the v_1
467 represents the 43% of the total area, v_2 14%, v_3 32%, v_4 9% and v_5 2%.

468 The highest values (v_4 and v_5) mainly occur in the western part of the region and, although
469 they are also present, to a lesser extent, in the north eastern part, where fluvial lacustrine
470 and terrigenous rocks prevail. The final reclassified grid (Rg_v) shows a v_1 equal to 34% of the
471 total area, v_2 38%, v_3 20%, v_4 6% and v_5 2%. The five classes of roughness show a good
472 correspondence with the geological substrate, with the highest values belonging to the
473 Carbonate complex and to some portions of the Terrigenous one. On the contrary the lowest
474 values are distributed on the alluvial and fluvial-lacustrine deposits. The low values on the
475 flat or gentle hillslope areas, although quite common, are a consequence of the DEM
476 resolution and accuracy. The quality of the elevation model is not high enough to well
477 represent the roughness of these areas. It is noteworthy, however, that high resolution
478 DEMs are not easily available for large areas, with extents comparable to the study area.
479 Therefore, the choice of using a DEM with a coarser resolution to derive roughness appears
480 to be a good compromise complementing the aim of the analysis and the data available for a
481 regional evaluation.

482 As for the percentage presence of Spv they are as follows: v_1 , 4% of the total area; v_2 , 1%;
483 v_3 , 3%; v_4 , 47%; v_5 , 45%. The Lcv shows the lowest variety; both v_1 and v_2 only cover 5%; v_3
484 covers 18%, v_4 31% and v_5 the remaining 40%. It is worth noting that Sp and Lc show the
485 highest percentages in the upper classes of variety relative to the other parameters in the
486 Gml equation (Eq. 1). The different trend of the variables depends on the neighbouring area
487 used for their estimation. For each variable the radius of the moving window is a
488 consequence of the observed spatial distribution of the variables. The opposite trend
489 rebalances the effects of the first three addends (geology, drainage density and roughness).
490 The final Gml map (Fig. 5a) is the result of the application of eq. (1). The dataset is in a grid
491 format with a cell size of 500m. The coarser resolution, in comparison to the data entry cell
492 size equal to 25x25m, is due to the Drainage density map, obtained at a 500m resolution.
493 The values of the output grid (Gml) range from a minimum of 5 to a maximum of 25. Cells
494 with value equal to 5 correspond to the minimum variety for all the input parameters; values
495 equal to 25 indicate that all the terrain data show the maximum variety. In the range 5-25 all
496 the possible combinations are present.

497 The Gml grid was classified into 5 classes according to Jenk's algorithm, similarly to all the
498 previous reclassification done on the data entries. As shown in Fig. 6, the index distribution
499 is strictly linked to the topographic arrangement: where the amplitude of relief is high the
500 Gml shows the highest values; on the contrary, the lowest value uniformly characterizes the
501 main flat areas of the region.



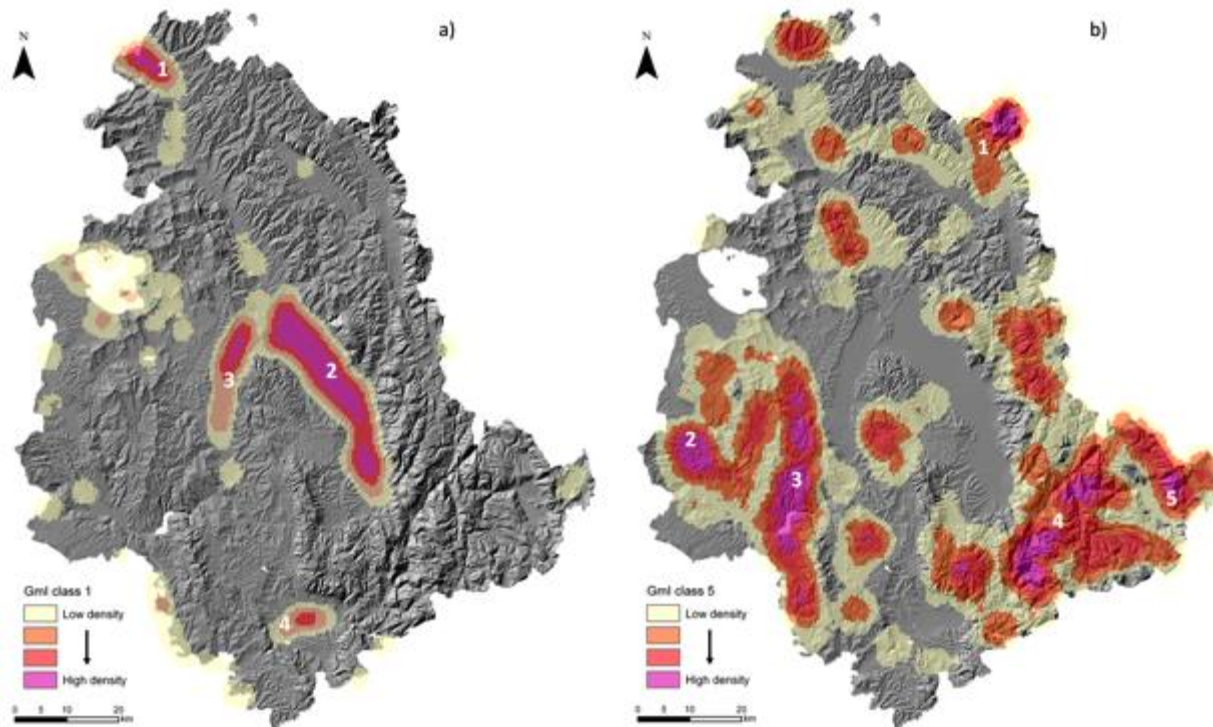
502

503 Figure 6. Geomorphodiversity Index (Gml) map. The value of Gml increases from 1

504 (lowest) to 5 (highest).

505

506 However, this trend is not observed everywhere and some further considerations must be
507 made. In order to better highlight the areas where the Gml reaches the lowest and the
508 highest values (class 1 and class 5 respectively) the two classes were extracted from the
509 Gml total grid, thus obtaining two grids representing class 1 and class 5. Each of the two
510 grids was converted to a point vector layer allowing the usage of a density point tool to
511 generate a density map. The density was calculated for the points falling in a
512 neighbourhood. If no points fall into the moving window, a NoData value is assigned to the
513 output cell. The density value is directly proportional to the number of points falling into the
514 mask. Lowest Gml values (Fig. 7a, class 1, 5% of the total area) cover a large areal extent
515 and correspond to the central part of the main intermontane basins, i.e. the northern part of
516 the Upper Tiber Valley (number 1 in Fig. 7a), the Umbrian Valley (number 2 in Fig. 7a) and
517 along the opposite segment of the Tiber Basin Valley (number 3 in Fig. 7a) as well as in the
518 Terni basin (number 4 in Fig. 7a).



519
 520 Figure 7. Maps of the spatial density of the Gml values belonging to: a) Class 1
 521 (lowest values of Gml); b) Class 5 (highest values of Gml).

522
 523 However, it is worth noting that the portion coincident with the class 1 of Gml is always
 524 limited to the center of the basins, whereas the index value increases towards the edges. It
 525 is important to note also that the lowest value is not so widespread in the Gubbio basin and
 526 on the flat uplands of the eastern regional limits; here the class 2 (12% of the total area) is
 527 present. In both cases the plain areas are less wide than in the Tiber basin segments.
 528 Consequently, the increase of the Gml value can be interpreted as the result of the close
 529 proximity of the mountain ridges bordering the basins. The abrupt change in energy relief
 530 along the transition between mountains and plains, usually occurring along a normal fault
 531 system, is responsible for the diversity of the geological component and, above all, of the
 532 topographic setting. The spatial irregularity of these components is again the main cause of

533 the abiotic diversity. The Gml classes 3 and 4 (respectively 37% and 38%) are equally
534 distributed on the hilly areas and on some portions of the mountainous areas.

535 The most meaningful result is the spatial distribution of the density map of class 5 (Fig. 7b),
536 which shows a very good agreement with the locations of the sites having the greatest
537 natural importance in the study area. Five main areas of interest, characterized by the
538 highest values of density, are detected. In the northern part of the Umbria region the first
539 relevant area is identified in the Mt. Cucco Regional Park area (number 1 in Fig. 7b). This
540 protected area is known as the 'womb of the Apennines' with a complex hypogean system
541 and karst phenomena (Gregori et al., 2005). Moreover, here some very particular geosites
542 are present due to the complex interaction between slope evolution and geomorphic
543 processes. In the central and southern portions of the Umbria region, moving from west to
544 east the other main relevant areas are present. In the western sector the zone between
545 Allerona, Fabro and Ficulle (number 2 in Fig. 7b) is famous for the badlands covering large
546 areas, creating an amazing landscape, not so common in the Umbria region. Then, moving
547 eastward a belt elongated north south is present around the Corbara Lake (number 3 in Fig.
548 7b). The Tiber River crosses the area along the Forello Gorge. As said above, this zone is
549 meaningful for the geomorphological evolution of the entire regional territory: a fault system
550 created the valley deflecting the Tiber River path in the lower Pleistocene. According to this
551 tectonic evolution, the entire area is very far from an equilibrium condition, for both the river
552 drainage network and the slope assessment. Therefore, the geomorphological evolution is
553 active and well evident. The remaining two areas characterized by high-density values of the
554 highest Gml class are located in the Carbonate complex, corresponding to the mountainous
555 part of the Umbria region. One of these zones (number 4 in Fig. 7b) is part of the Valnerina,

556 a valley well known for being one of the best tourist destinations due to its natural values.
557 The maximum density partially coincides with the extent of the “Valnerina geologic park and
558 Geologic Study Centre”. Geosites and geomorphosites are present in this park, as well as
559 georoutes. The last area (number 5 in Fig. 7b) is surrounded by the National Park of the
560 Sibillini Mountains. The zone (700 km²) is the only national park present in the Umbria region
561 (Fig. 8).



562
563 Figure 8. Pian Grande with Mt. Vettore in the background (left). In the foreground the
564 Mergani River (photo by G. Mulazzano).

565
566 It contains some geological uniqueness including polije, karstic features and fluvial
567 landforms (alluvial fans). Moreover, the area is enriched with spectacular glacial (glacial
568 cirque) and periglacial (stratified talus slope deposits e.g. grèze litée) landforms dated to the

569 Middle Pleistocene and now involved in mass wasting phenomena (Della Seta et al., in
570 press).

571

572 6. Validation

573 In order to validate the results a comparison with a geomorphological digital map was
574 performed.

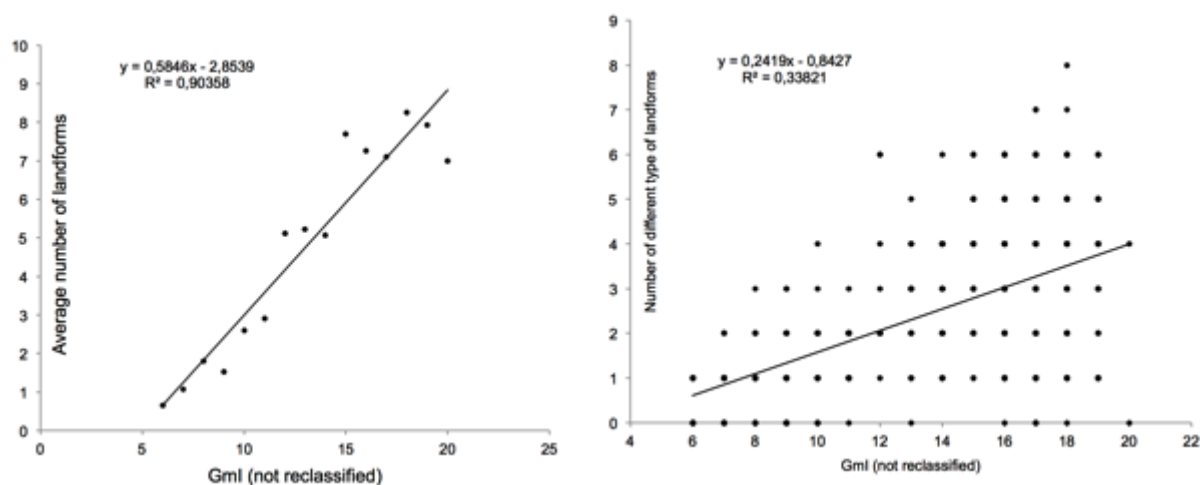
575 In the geomorphological digital dataset each landform is modelled as a vector (point, polyline
576 or polygon) with an attribute table where the type of feature and the process responsible for
577 each landform are always mentioned. The vector geomorphological map was converted to a
578 raster dataset, with a cell size of 50m, in order to compute the landform multiplicity (focal
579 statistics tool in the software ArcGIS) and compare it with the geodiversity index map. The
580 landform assortment was computed considering i) the number of landforms and ii) the
581 number of landform types, in a 1 km² circle neighbourhood.

582 The relation between the number of landforms of the geomorphological map and the values
583 of the Gml was evaluated using the Zonal Statistics tool in GIS, in order to quantify the
584 capability of the GI to detect the geomorphological diversity of the area.

585 The validation was tested in a portion of the Upper Tiber Valley (Sansepolcro sub-basin, Fig.
586 1) where the Gml shows the lowest value of diversity. The area is an intermontane basin
587 with a width of up to 4,500 m, completely covered by the Tiber River alluvial deposits and
588 infilled with tens of meters of Holocene alluvial deposits. The eastern boundary is
589 characterized by a “bajada” of large alluvial fans; along the western boundary alluvial
590 terraces are present. The normal faults activity bordering the basin generated an intensive
591 subsidence (Melelli et al., 2014). The morphological arrangement is a large flat area whose

592 monotony is interrupted only near the bordering limits. This area was chosen as a test area
593 in order to observe if, despite the presence in the geomorphological map of a certain number
594 of fluvial and tectonic landforms, the correlation between presence/absence of features and
595 Gml is verified.

596 In Fig. 9 the positive correlation between Gml and the average number of landforms is
597 shown. Moreover, the comparison between the Gml and the number of different types of
598 landforms is also displayed.



599

600 Figure 9. Results of the validation. Relationships between: (left) Gml and average
601 number of landforms; (right) Gml and number of different types of landforms.

602

603 The result, in both cases, is: the greater the index, the greater the number and the range of
604 landforms. To conclude, the outcomes of the validation analysis indicate that the Gml index
605 is capable of representing very well and with a high degree of accuracy the diversity of
606 landforms occurring in the study area.

607

608 7. Discussion

609 The algorithm proposed in this work is inspired to the expression proposed by Serrano and
610 Ruiz-Flaño (2007), where the geodiversity index is computed as the multiplication between
611 N and R, divided by $\ln S$. In this formula N is the arithmetic sum of the physical elements, R
612 is the roughness and S is the real surface. The Naperian logarithm is introduced to
613 normalize the result with the area of the unit. In the equation proposed here (Eq. 1) only the
614 arithmetic sum of the physical elements is taken into account. The reason is that in this work
615 only the geomorphodiversity is evaluated; therefore, the morphometric parameters are
616 regarded as the most important for the analysis. The only parameter, which is not strictly
617 morphometric, is the geological factor. The choice of considering this parameter is based on
618 the consideration that the lithotypes affect the response of the relief to the geomorphic
619 agents, and, consequently, of the resulting landforms. All the input parameters are strictly
620 related to the morphology of the surface. To compute the geomorphodiversity, we assumed
621 that all of them have the same weight since the grids of their variety are added to each
622 other, once reclassified in the same number of classes. For that reason the roughness is
623 simply added, and not multiplied, to the other factors. We neglected the natural logarithm of

624 the cell size because the analysis is confined to the invariable medium-scale of horizontal
625 resolution of the DEMs used.

626 The main advantage of this formula is that the diversity of each input data is already a
627 measure of the diversity of the abiotic components. This is a very important point because
628 we do not simply sum a quantity as is commonly done in most of the previous scientific
629 approaches. The focal function allows measuring the variety in well-defined surrounding
630 areas, thus converting the initial terrain information to an intermediate step, which leads to
631 treat the data in terms of 'diversity'. Moreover, the source of the input data (except for the
632 geological layer) is the grid DEM. The great availability of DEMs derived from remote
633 sensing allows analysing large areas, whilst terrain data (as geomorphological or geological
634 dataset) are not always available and not always uniform. However, the quality of DEMs
635 analysis depends on the spatial resolution. In particular some of the input parameters in Eq.
636 1 depend on the scale of analysis; these include the roughness, the slope classification and
637 the landform classification. A good compromise to minimize this problem is to restrict the
638 analyses to the scale range typical of meso-scale features, i.e. from few tens of meters to
639 some hundreds of meters. According to this limit the DEMs cell size is selected with a
640 medium resolution, capable to guarantee the required precision needed for the application of
641 the method.

642 We validated the method using traditional geomorphological maps, although these thematic
643 maps are excluded as input data. The aim is to compare the qualitative classification of the
644 landscape based on landforms and shaping processes with the quantitative method
645 proposed. The good spatial correlation reported between the geomorphodiversity index

646 values, the number of landforms and with the number of different types of landforms seems
647 to confirm the quality and robustness of the proposed quantitative approach.

648 The Gml index is inspired to the previous ones proposed in the scientific literature (Benito-
649 Calvo et al., 2009; Hjort and Luoto, 2010; Pereira et al., 2013; Serrano and Ruiz-Flaño,
650 2007; Zwoliński, 2010). Some similarities may be underlined, that is the spatial analysis in a
651 GIS system and the raster format preferred for the data input. However this index has two
652 main differences compared to the other numerical methods. The first is that in the final sum
653 of the formula the single addends do not derive from a sum of a quantity of elements (i.e. the
654 number of geological lithotypes outcropping in a pixel) as in many other formulations (Hjort
655 and Luoto, 2010; Pereira et al., 2013; Zwoliński, 2010). In this formula the addends are grids
656 with values from 1 to 5 measuring the variety of the input parameter. This way a specific
657 focal function is used with the aim of evaluating the diversity in each pixel (or cell). The
658 second main difference is that the proposed method, with the exception of the geological
659 layer, takes advantage of Digital Elevation Models for deriving all the input parameters.
660 Digital Elevation Models are widely accessible for large areas and often available for free
661 downloading. Starting from the topographic signature allows releasing the index from
662 thematic maps that are not always available to reproduce the method in different geographic
663 regions.

664 Moreover, comparing the geomorphodiversity with the method for delimiting the
665 physiographic units could highlight some important points of convergence between the two
666 concepts as much as substantial differences. The quantitative procedure proposed in this
667 work and the results in terms of spatial diversity may be, in our opinion, a valuable
668 parameter to be considered in the definition of the physiographic units.

669

670 8. Conclusions

671 The natural heritage is one of the most important wealth in many areas of the Earth surface.

672 The diversity of natural ecosystems manifests itself as biodiversity and geodiversity, which

673 are mutually dependant. The topographic surface, where the geomorphic agents are acting,

674 is the layer where the abiotic and the biotic elements interact; at the same time, it is the

675 constraint for the geomorphological evidence.

676 Geomorphodiversity is the aspect of geodiversity associated with the geomorphological

677 diversity or the quantity and number of types of landforms.

678 A quantitative evaluation in GIS requires digital data as input parameters. Landforms are

679 generally represented in geomorphological maps as objects in a vector format deriving from

680 a semantic approach. According to this method, a landform is the result of a classification

681 that simplifies the “real world”, depending on the scientists’ background and the research

682 context.

683 However, the need to classify the landscape in well-defined shapes can lead to some

684 limitation if the traditional mapping techniques are used. The geomorphological maps show

685 a high heterogeneity in terms of graphical techniques used for the cartographic output. The

686 map scale involves subjective choices for landform representation and localization. These

687 limits strongly affect the extent and the shape of each single landform represented on a

688 map. Therefore the landform representation depends on the scale and may be depicted with

689 a point, a polyline or a polygon, thus varying the spatial extent of the input data and their

690 consequent weight in the spatial analysis.

691 Based on these considerations, the use of a geometric approach like the one proposed in
692 this work should be preferred. In this approach, extracting the topographic primary and
693 secondary attributes from the terrain data performs the analysis of the morphological input
694 factors. The range, the ranking and the spatial distribution of these topographic attributes
695 allow classifying the morphology using an unbiased method.

696 The high correspondence between the physical landscape and the factors at the base of the
697 geomorphodiversity in the Umbria region confirms that the concept of geomorphodiversity is
698 another way to explore the physiography of a territory (Bailey, 2009; Fenneman, 1916). If on
699 one hand the geomorphodiversity excludes the biotic components and the human pressure,
700 on the other it includes all the fundamental variables that characterize the geomorphological
701 arrangement of an area. Since the geomorphological landforms and processes are strictly
702 linked to the geological evolution of an area, the proposed index may highlight, better than
703 other methods, the areas where the abiotic components are more active and are modifying
704 the landscape. This approach is particular meaningful in areas such as the Umbria region
705 where the endogenous and exogenous forces are still working to built a unique landscape in
706 which – quoting the French geographer H. Desplanches (1911-1983) – “the contrasts
707 overlap almost for fun”.

708

709 References

710 Basilici, G., 1997. Sedimentary facies in an extensional and deep-lacustrine depositional
711 system: the Pliocene Tiberino Basin, Central Italy. *Sedimentary Geology* 109(1), 73-94.

712 Bailey, R.G., 2009. *Ecosystem geography: from ecoregions to sites*. Springer Science &
713 Business Media.

714 Benito-Calvo, A., Pérez-González, A., Magri, O., Meza, P., 2009. Assessing regional
715 geodiversity: the Iberian Peninsula. *Earth Surface Processes and Landforms* 34(10), 1433-
716 45.

717 Bétard, F., 2013. Patch-Scale Relationships Between Geodiversity and Biodiversity in Hard
718 Rock Quarries: Case Study from a Disused Quartzite Quarry in NW France. *Geoheritage*
719 5(2), 59-71.

720 Carton, A., Coratza, P., Marchetti, M., 2005. Guidelines for geomorphological sites mapping:
721 examples from Italy. *Geomorphologie* 2, 209-18.

722 Ciotoli, G., Della Seta, M., Del Monte, M., Fredi, P., Lombardi, S., Lupia Palmieri, E.,
723 Pugliese, F., 2003. Morphological and geochemical evidence of neotectonics in the volcanic
724 area of Monti Vulsini (Latium, Italy). *Quaternary International* 101, 103-13.

725 Della Seta, M., Melelli, L., Pambianchi, G. (in press). Reliefs, intermontane basins and
726 civilization in the Umbria-Marche Apennines: origin and life by geological consent. In:
727 *Landscapes and Landforms of Italy*, edited by M. Soldati and M. Marchetti. New York:
728 Springer.

729 Del Monte, M., 1996. Rapporti tra caratteristiche morfometriche e processi di denudazione
730 nel bacino idrografico del Torrente Salandrella (Basilicata). *Geologica Romana* 32, 151-65.

731 De Reu, J., Bourgeois, J., Bats, M., Zwertvaegher, A., Gelorini, V., De Smedt, P., Chu, W.,
732 Antrop, M., De Maeyer, P., Finke, P., Van Meirvenne, M., Verniers, J., Crombé, P. 2013.
733 Application of the topographic position index to heterogeneous landscapes. *Geomorphology*
734 186, 39-49.

735 Erikstad, L., 2013. Geoheritage and geodiversity management: the questions for tomorrow.
736 Proceedings of the Geologists' Association 124(4), 713-19.

737 Evans, I.S., 2013. Land surface derivatives: history, calculation and further development.
738 Proceedings of geomorphometry, 16-20.

739 Fenneman, N.M., 1928. Physiographic divisions of the United States. Annals of the
740 Association of American Geographers, 18(4), 261-353.

741 Ferrero, E., Giardino, M., Lozar, F., Giordano, E., Belluso, E., Perotti L., 2012. Geodiversity
742 action plans for the enhancement of geoheritage in the Piemonte region (north-western
743 Italy). Annals of Geophysics 55(3), 487-95.

744 Gordon, J.E., Barron, H.F., Hansom, J.D., Thomas, M.F., 2012. Engaging with geodiversity-
745 why it matters. Proceedings of the Geologists' Association 123(1), 1-6.

746 Gray, M., 2004. Geodiversity valuing and conserving abiotic nature. Chichester, U.K.: John
747 Wiley & Sons Ltd.

748 Gregori, L., Melelli, L., Rapicetta, S., Taramelli, A., 2005. The main Geomorphosites in
749 Umbria. Il Quaternario 1(8), 93-101.

750 Gustavsson, M., Kolstrup, E., Seijmonsbergen, A.C. 2006. A new symbol-and-GIS based
751 detailed geomorphological mapping system: Renewal of a scientific discipline for
752 understanding landscape development. Geomorphology 77(1), 90-111.

753 Guzzetti, F., Reichenbach, P. 1994. Towards a definition of topographic divisions for Italy.
754 Geomorphology 11(1), 57-74.

755 Hani, A.F.M., Sathyamoorthy, D., Asirvadam, V.S., 2011. A method for computation of
756 surface roughness of digital elevation model terrains via multiscale analysis. *Computers &*
757 *Geosciences* 37(2), 177-92.

758 Hjort, J., Heikkinen, R.K., Luoto, M. 2012. Inclusion of explicit measures of geodiversity
759 improve biodiversity models in a boreal landscape. *Biodiversity and Conservation* 21(13),
760 3487-506.

761 Hjort, J., Luoto, M. 2010. Geodiversity of high-latitude landscapes in northern Finland.
762 *Geomorphology* 115(1-2), 109-16.

763 Hollaus, M., Aubrech C., Höfle, B., Steinnocher, K., Wagner, W., 2011. Roughness mapping
764 on various vertical scales based on full-waveform airborne laser scanning data. *Remote*
765 *Sensing* 3(3), 503-23.

766 Hooson, D.J., 1968. The development of geography in pre-Soviet Russia. *Annals of the*
767 *Association of American Geographers*, 58(2), 250-272.

768 Horton, R.E., 1945. Erosional development of streams and their drainage basins:
769 hydrophysical approach to quantitative morphology. *Geological Society of America Bulletin*
770 56, 275–370.

771 Jenks, G.F., 1967. The Data Model Concept in Statistical Mapping. *International Yearbook*
772 *of Cartography* 7, 186-90.

773 Jenness, J.S., 2004. Calculating landscape surface area from digital elevation models.
774 *Wildlife Society Bulletin* 32(3), 829-39.

775 Lupia Palmieri, E., Centamore, E., Ciccacci, S., D'Alessandro, L., Del Monte, M., Fredi, P.,
776 Pugliese, F., 2001. Geomorfologia quantitativa e morfodinamica del territorio abruzzese. III -
777 Il bacino idrografico del Fiume Saline. *Geografia Fisica e Dinamica Quaternaria* 24(2), 157-
778 76.

779 Margottini, C., Melelli, L., Spizzichino, D. (in press). The tuff cities: a "living landscape" at the
780 border of volcanoes in central Italy. In: *Landscapes and Landforms of Italy*, edited by M.
781 Soldati and M. Marchetti. New York: Springer.

782 Martinez-Graña, A.M., Goy, J.L., Cimarra, C., 2014. 2D to 3D geologic mapping
783 transformation using virtual globes and flight simulators and their applications in the analysis
784 of geodiversity in natural areas. *Environmental Earth Sciences*. DOI 10.1007/s12665-014-
785 3959-1.

786 Matthews, T.J., 2014. Integrating Geoconservation and Biodiversity Conservation:
787 Theoretical Foundations and Conservation Recommendations in a European Union Context.
788 *Geoheritage*, 6(1), 57-70.

789 Melelli, L., 2014. Geodiversity: a new quantitative index for natural protected areas
790 enhancement. *GeoJournal of Tourism and Geosites* 13(1), 2-12.

791 Melelli, L., Gregori, L., Mancinelli, L., 2012. The Use of Remote Sensed Data and GIS to
792 Produce a Digital Geomorphological Map of a Test Area in Central Italy. In *Remote Sensing*
793 of Planet Earth, 97-116, edited by Y. Chemin. Rijeka, Croatia: InTech.

794 Melelli, L., Pucci, S., Saccucci, L., Mirabella, F., Pazzaglia, F., Barchi, M., 2014.
795 Morphotectonics of the Upper Tiber Valley (Northern Apennines, Italy) through quantitative

796 analysis of drainage and landforms. *Rendiconti Lincei* 25(2), 129-38.

797 Melelli, L., Taramelli, A., 2010. Criteria for the elaboration of susceptibility maps for DGSD
798 phenomena in central Italy. *Geografia Fisica e Dinamica Quaternaria* 33(2), 179-85.

799 Miliaris, G.C., Argialas, D.P., 1999. Segmentation of physiographic features from the
800 global digital elevation model/GTOPO30. *Computers & Geosciences*, 25(7), 715-728.

801 Musila, W., Todt, H., Uster, D., Dalitz, H., 2005. Is Geodiversity Correlated to Biodiversity? A
802 Case Study of the Relationship Between Spatial Heterogeneity of Soil Resources and Tree
803 Diversity in a Western Kenyan Rainforest. In: *African Biodiversity*, 405-14, edited by B.A.
804 Huber et al. Netherlands: Springer.

805 Panizza, M., Piacente, S., 2009. Cultural geomorphology and geodiversity. In
806 *Geomorphosites*, 35-48, edited by Reynard E., Coratza P. and Regolini-Bissig G. Munich:
807 Pfeil Verlag.

808 Peccerillo, A., 2005. Plio-quaternary volcanism in Italy, Berlin, Heidelberg: Springer-Verlag.

809 Pereira, D.I., Pereira, P., Brilha, J., Santhos, L., 2013. Geodiversity Assessment of Paraná
810 State (Brazil): An Innovative Approach. *Environmental Management* 52(3), 541-52.

811 Pike, R.J., 2000. Geomorphometry-diversity in quantitative surface analysis. *Progress in*
812 *Physical Geography* 24(1), 1-20.

813 Reynard, E., Coratza, P., 2007. Geomorphosites and geodiversity: a new domain of
814 research. *Geographica Helvetica* 62, 138–39

815 Ruban, D.A., 2010. Quantification of geodiversity and its loss. *Proceedings of the Geologists'*

816 Association 121(3), 326-33.

817 Serrano, E., Ruiz-Flaño, P., 2007. Geodiversity: a theoretical and applied concept.”
818 *Geographica Helvetica* 62, 140–147.

819 Silva, J.dP., Rodrigues, C., Pereira, D.I., 2015. Mapping and Analysis of Geodiversity
820 Indices in the Xingu River Basin, Amazonia, Brazil. *Geoheritage* 7, 337-50.

821 Strahler, A.N., 1958. Dimensional analysis applied to fluvially eroded landforms. *Geological*
822 *Society of America Bulletin* 69, 1117-42.

823 Taramelli, A., Melelli, L., 2009a. Detecting alluvial fans using quantitative roughness
824 characterization and fuzzy logic analysis using the Shuttle Radar Topography Mission data.
825 *International Journal of Computer Science and Software Technology* 2(1), 55-67.

826 Taramelli, A., Melelli, L., 2009b. Map of deep seated gravitational slope deformations
827 susceptibility in central Italy, derived from SRTM DEM and spectral mixing analysis of the
828 Landsat ETM+ data. *International Journal of Remote Sensing* 2(30), 357-87.

829 Taramelli, A., Reichenbach, P., Ardizzone F., 2008. Comparison of SRTM elevation data
830 with cartographically derived DEMs in Italy.” *Revista Geográfica Acadêmica* 2(8), 41-52.

831 Thomas, M.F. 2012. A geomorphological approach to geodiversity – its applications to
832 geoconservation and geotourism. *Quaestiones Geographicae* 31(1), 81-89.

833 Tucker, G.E., Catani, F., Rinaldo A., Bras R.L. 2001. Statistical analysis of drainage density
834 from digital terrain data. *Geomorphology* 36(3), 187-202.

835 Vergari, F., 2009. Valutazione della geodiversità mediante applicazioni GIS. ISPRA,

- 836 Quaderni - Educazione e Formazione Ambientale n. 1/2009, ISBN 978-88-448-0408-4.
- 837 Yongxin, D., 2007. New trends in digital terrain analysis: landform definition, representation,
838 and classification. *Progress in Physical Geography* 31(4), 405-19.
- 839 Weiss, A., 2001. Topographic Position and Landforms Analysis. ESRI User Conference, San
840 Diego, CA.
- 841 Wu, S., Li, S., Huang, G.H., 2008. A study on DEM-derived primary topographic attributes
842 for hydrologic applications: Sensitivity to elevation data resolution. *Applied Geography* 28,
843 210-223.
- 844 Zwoliński, Z., 2010. The routine of landform geodiversity map design for the Polish
845 Carpathian Mts. *Landform Analysis* 11, 77-85.
- 846

847 Captions

848 Figure 1. Umbria region: location map and elevation ranges a.s.l. 1) <200m, 2) 200-
849 500m a.s.l., 3) 500-800m, 4) >800m.

850

851 Figure 2. Correspondence between slope angle values and lithological complexes.
852 Slope angle classes: 1) 0°-5°, 2) 5°-16°, 3) 16°-30°, 4) >30°. Lithological complexes:
853 5) Fluvial lacustrine deposits, 6) Volcanic complex, 7) Terrigenous complex, 8)
854 Carbonate complex.

855

856 Figure 3. Flow chart showing the steps of the analysis.

857

858 Figure 4. Variety maps in grid format. a) Geological factor, b) Drainage density, c)
859 Roughness, 5) Slope position, 6) Landform category. Colours indicate the variety,
860 which increases from class v1 (lowest) to class v5 (highest).

861

862 Figure 5. Pie charts showing the percentages of each variety class for the maps
863 shown in figure 4. a) Geological factor, b) Drainage density, c) Roughness, 5) Slope
864 position, 6) Landform category. The colours indicate the variety which increases from
865 class v1 (lowest) to class v5 (highest).

866

867 Figure 6. Geomorphodiversity Index (Gml) map. The value of Gml increases from 1
868 (lowest) to 5 (highest).

869

870 Figure 7. Maps of the spatial density of the Gml values belonging to: a) Class 1
871 (lowest values of Gml); b) Class 5 (highest values of Gml).

872

873 Figure 8. Pian Grande with Mt. Vettore in the background (left). In the foreground the
874 Mergani River (photo by G. Mulazzano).

875

876 Figure 9. Results of the validation. Relationships between: (left) Gml and average
877 number of landforms; (right) Gml and number of different types of landforms.

Figure1
[Click here to download high resolution image](#)

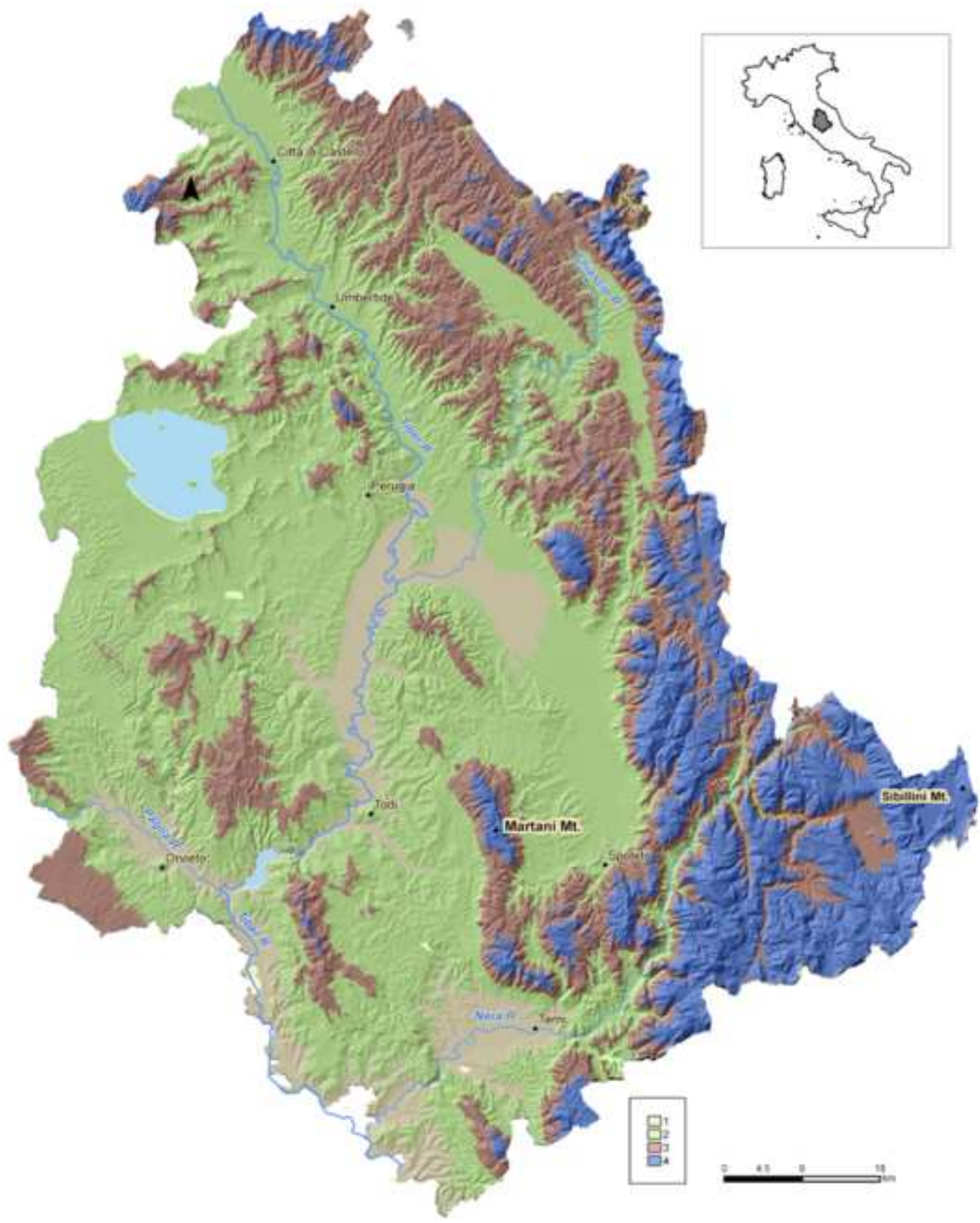


Figure2
[Click here to download high resolution image](#)

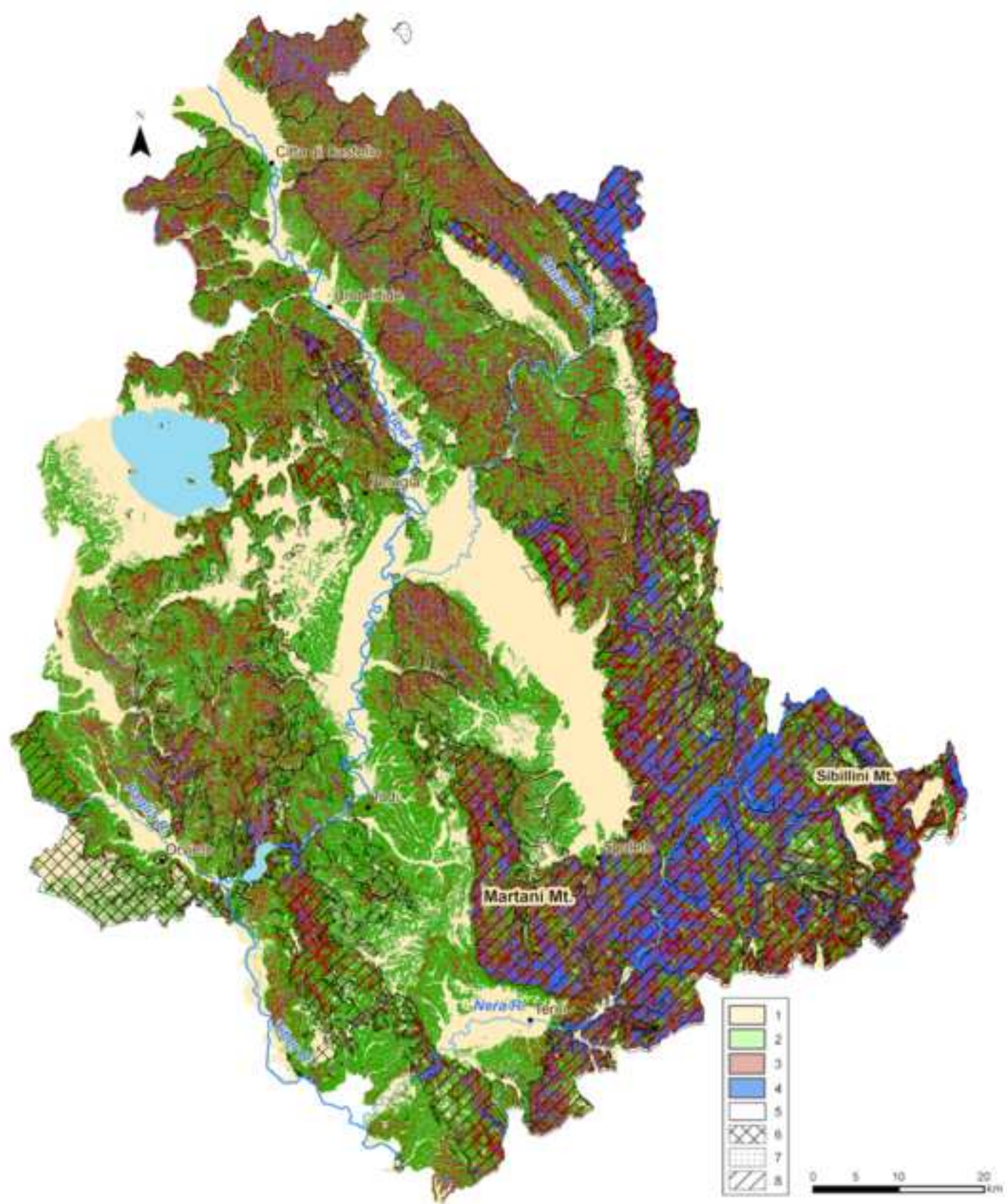


Figure3
[Click here to download high resolution image](#)

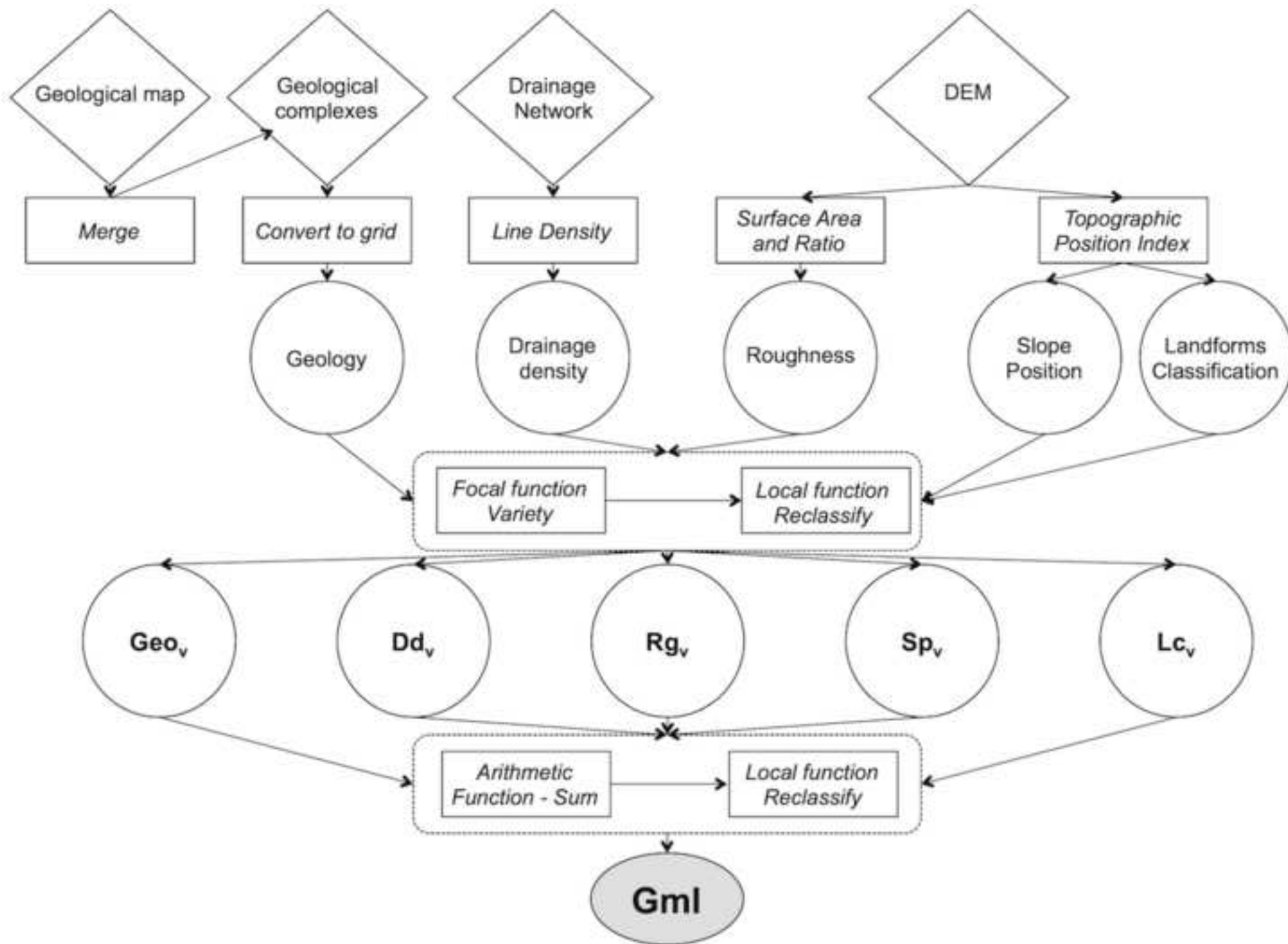


Figure4
[Click here to download high resolution image](#)

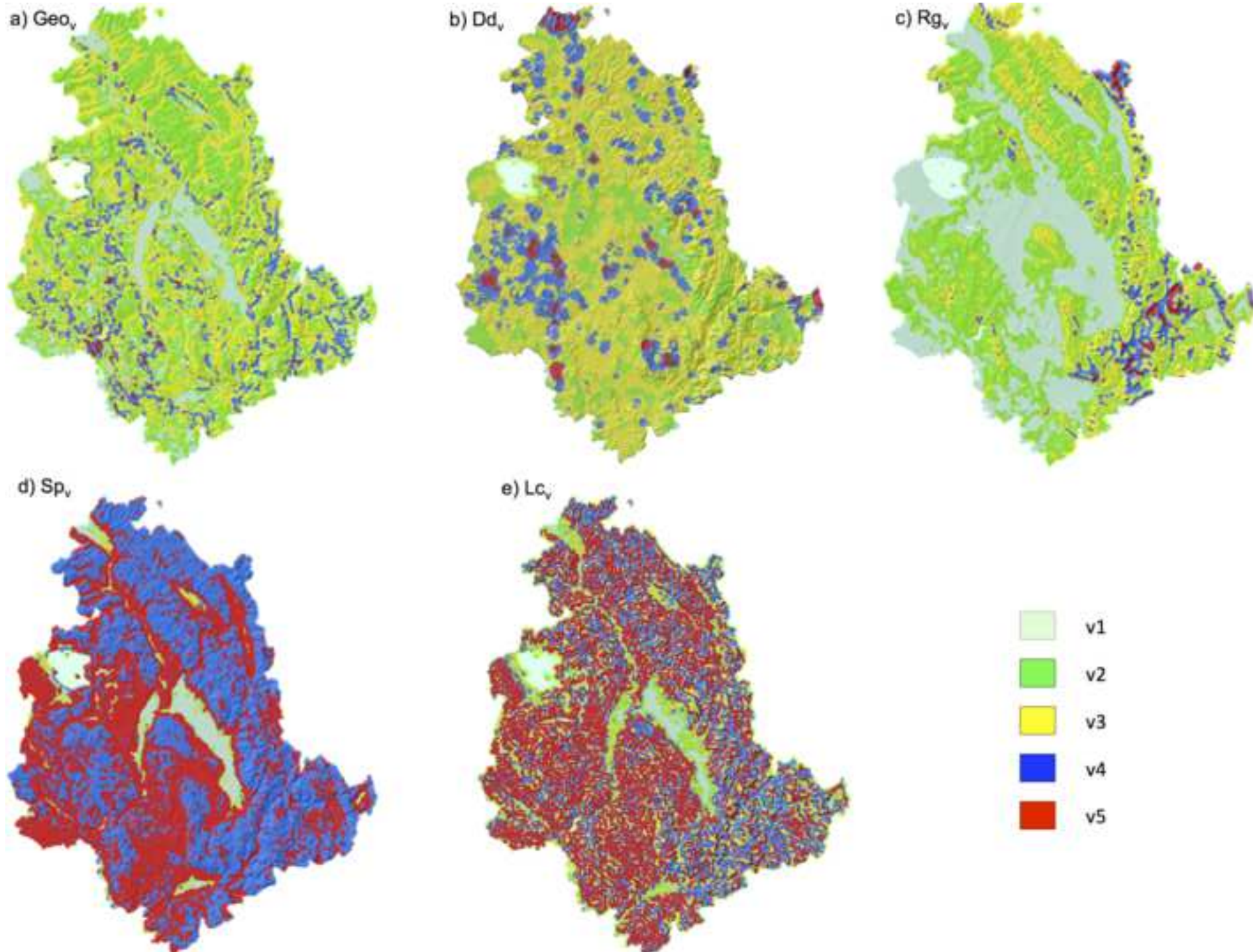
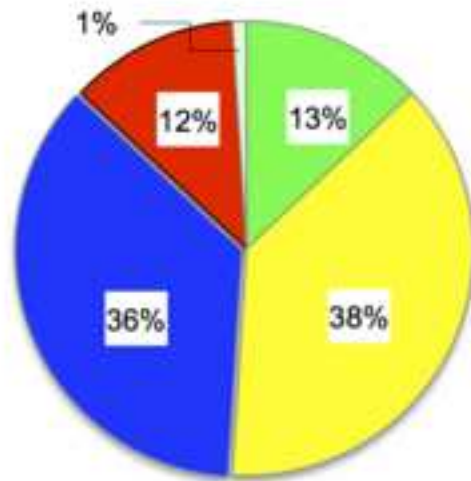


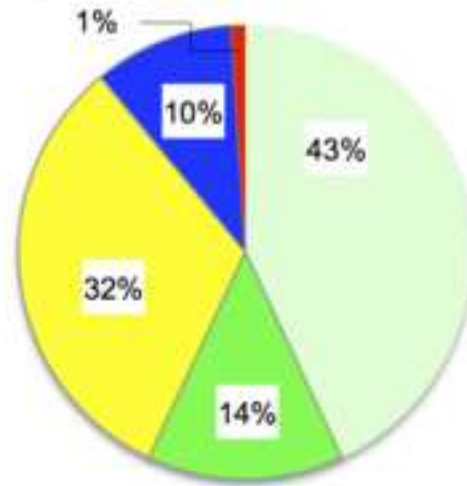
Figure5

[Click here to download high resolution image](#)

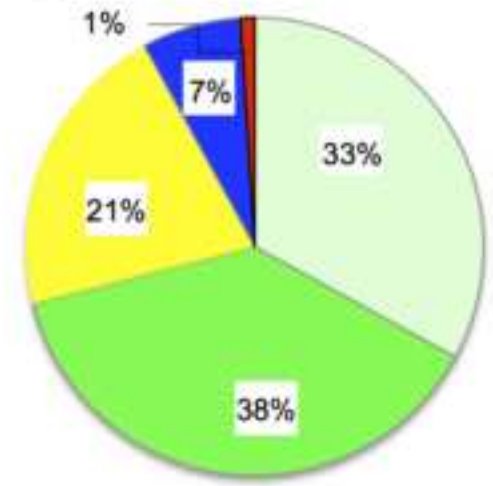
a) Geo_v



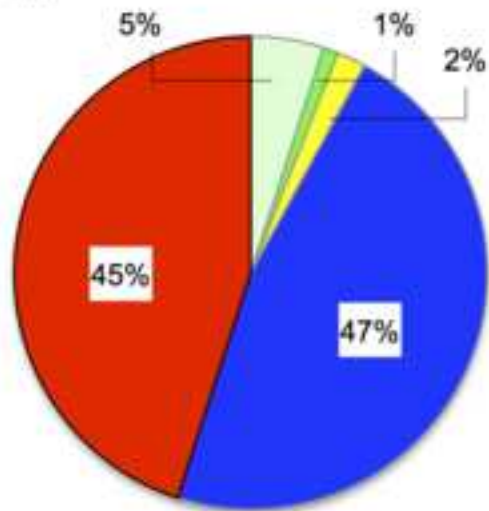
b) Dd_v



c) Rg_v



d) Sp_v



e) Lc_v

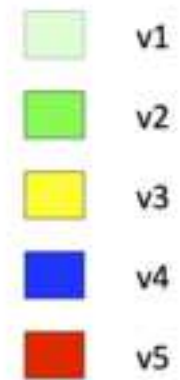
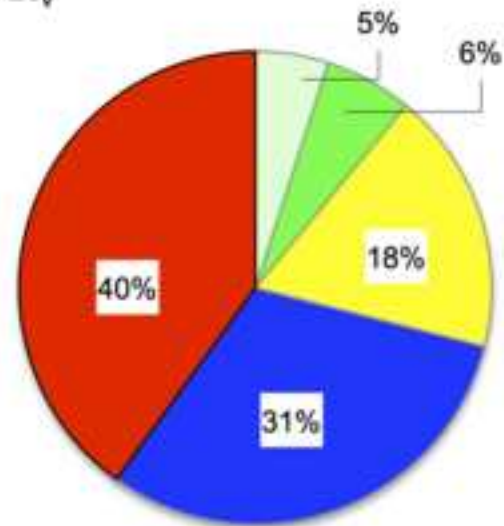


Figure6
[Click here to download high resolution image](#)

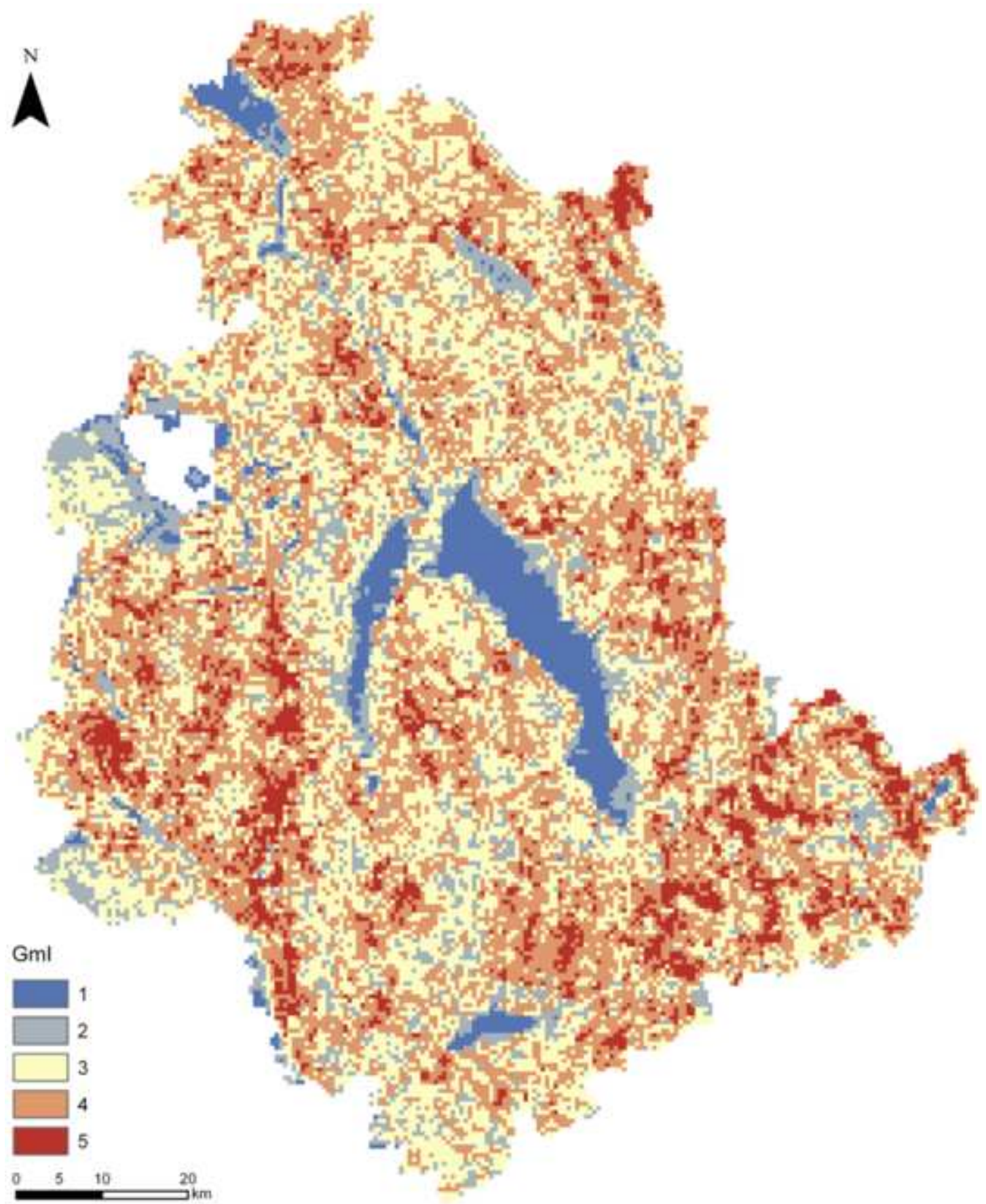


Figure7
[Click here to download high resolution image](#)

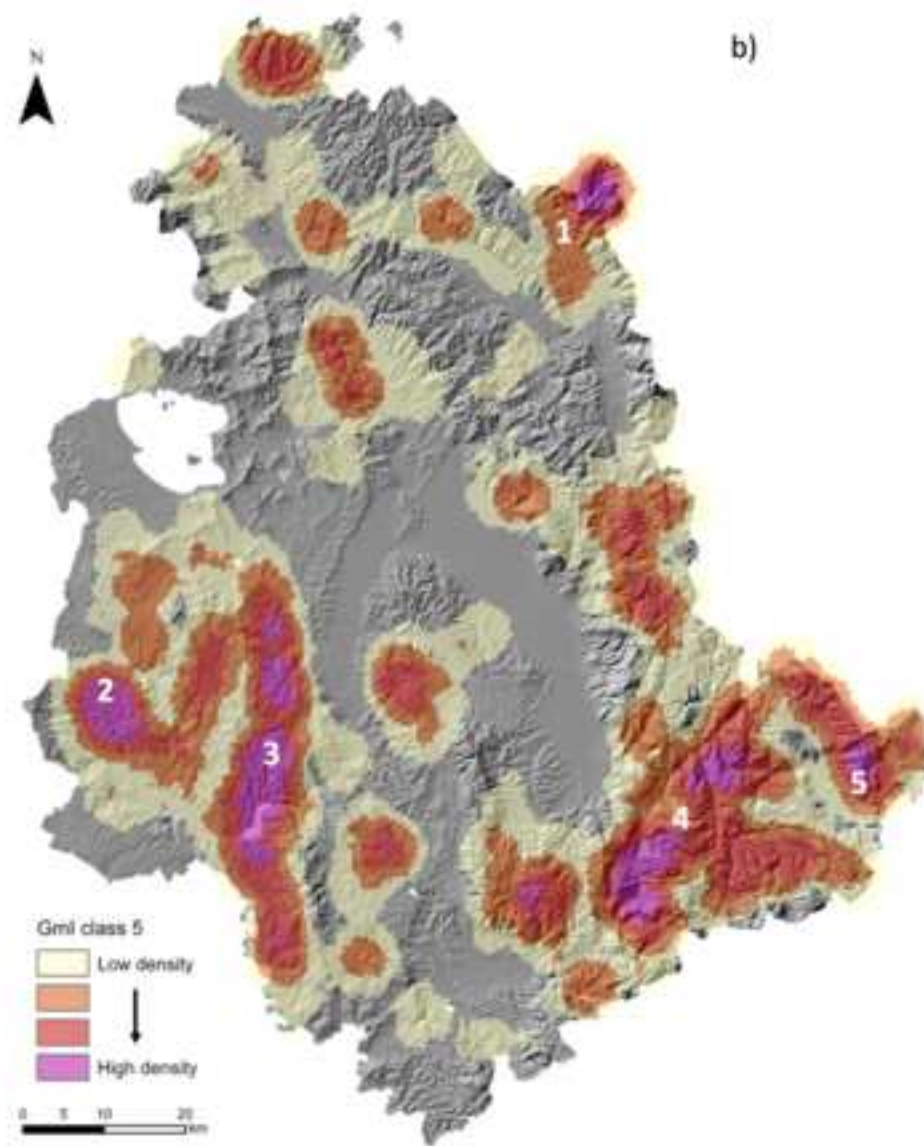
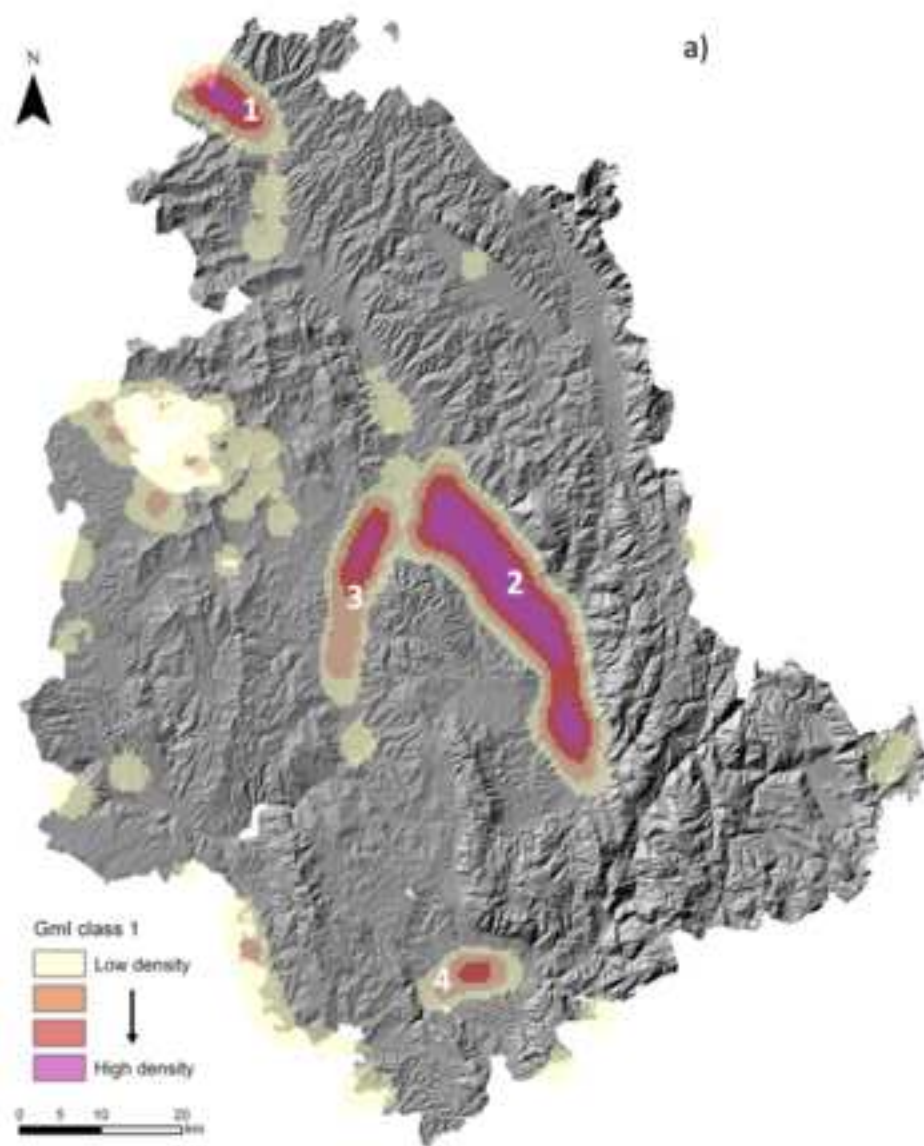


Figure8
[Click here to download high resolution image](#)



Figure9

[Click here to download high resolution image](#)

